Proteomic profiling of *Mycobacterium tuberculosis* culture filtrate identifies novel O-glycosylated proteins

Paula Tucci[1*], Madelón Portela[2,3], Carlos Rivas Chetto[4], Gualberto González-Sapienza[5], Mónica Marín[1]

[1] Sección Bioquímica, Facultad de Ciencias, Universidad de la República, Montevideo, Uruguay

[2] Unidad de Bioquímica y Proteómica Analíticas, Institut Pasteur de Montevideo, Montevideo, Uruguay

[3] Facultad de Ciencias, Universidad de la República, Montevideo, Uruguay

[4] Departamento de Laboratorio, Comisión Honoraria para la Lucha Antituberculosa y Enfermedades Prevalentes, Centro de Referencia Nacional para Micobacterias, Ministerio de Salud Pública, Montevideo, Uruguay.

[5] Cátedra de Inmunología, DEPBIO, Facultad de Química, Montevideo, Uruguay

* Corresponding autor

E-mail: ptucci@fcien.edu.uy (PT)

Abstract

Despite being the subject of intensive research, tuberculosis, caused by *Mycobacterium tuberculosis,* remains at present the leading cause of death from an infectious agent. Secreted and cell wall proteins interact with the host and play important roles in pathogenicity. These proteins have been explored as candidate diagnostic markers, potential drug targets or vaccine antigens, and special attention has been given to the role of their post-translational modifications. With the purpose of contributing to the proteomic characterization of this important pathogen including an O-glycosylation profile analysis, we performed a shotgun analysis of culture filtrate proteins of *M. tuberculosis* based on a liquid nano-HPLC tandem mass spectrometry and a label-free spectral counting normalization approach for protein quantification. We identified 1314 *M. tuberculosis* proteins in culture filtrate and found that the most abundant proteins belong to the extracellular region or cell wall compartment, and that the functional categories with higher protein abundance factor were virulence, detoxification and adaptation, and cell wall and cell processes. In culture filtrate, 140 proteins were predicted to contain one of the three types of bacterial N-terminal signal peptides. Besides, various proteins belonging to the ESX secretion systems, and to the PE and PPE families, secreted by the type VII secretion system using nonclassical secretion signals, were also identified. O-glycosylation was identified as a frequent modification, being present in 108 proteins, principally lipoproteins and secreted immunogenic antigens. We could identify a group of proteins consistently detected in previous studies, most of which were highly abundant proteins. Interestingly, we also provide proteomic evidence for 62 novel O-glycosylated proteins, aiding to the glycoproteomic characterization of relevant antigenic membrane and exported proteins.

Introduction

Mycobacterium tuberculosis, the causative agent of tuberculosis (TB) remains a major public health threat. According to the last Global Tuberculosis Report published by the World Health Organization (WHO) an estimate of 10 million people developed TB disease in 2017. Moreover, TB is at present the leading cause of death from a single infectious agent, causing an estimated 1.3 million deaths among HIV-negative people and approximately 300 thousand deaths among HIV-positive people [1]. Although TB diagnosis and successful treatment averts millions of deaths each year, there are still large and persistent gaps related to this infection that must be resolved in order to accelerate progress towards the goal of ending the TB epidemic endorsed by WHO [1].

M. tuberculosis (MTB), has evolved successful mechanisms to circumvent the hostile environment of the macrophage, such as inhibiting the phagosome-lysosome fusion and to escape the acidic environment inside the phagolysosome [2]. MTB may be unique in its ability to exploit adaptive immune responses, through inflammatory lung tissue damage, to promote its transmission [3]. It has been proposed that this microorganism was pressed by an evolutionary selection that resulted in an infection that induces partial immunity, where the host survives a long period after being infected with the pathogen, aiding in microorganism persistence and transmission [3]. MTB mechanisms of evasion of host immune system were proposed to have consequences in the design of TB vaccines [3] and to be in part responsible of the poor performance of immune-based diagnostic tools [4,5].

In that context, there is a pressing need to advance the knowledge of the mechanisms that mediate its virulence. Among the tools to study the biology of MTB, *M. tuberculosis* H37Rv is a well-characterized human lung isolate and one of the most commonly used laboratory strains of *M. tuberculosis*. This virulent strain has been used in several investigations to understand the molecular mechanisms of MTB virulence, pathogenicity and persistence, as it provides a unique

platform to investigate biochemical and signaling pathways associated with pathogenicity [6]. In particular, it has been extensively used to identify pathogen biomarkers of *M. tuberculosis* infection and disease. These are generally major components identified by electrophoresis and mass spectrometry both in total extracts and culture filtrates [7–9].

The cell envelope and secreted components of MTB are among the bacterial molecules most commonly described as potential biomarkers of the infection, or involved in host immune evasion. Mycobacteria possess a remarkably complex cell envelope consisting of a cytoplasmic membrane and a cell wall. These constitute an efficient permeability barrier that plays a crucial role in intrinsic drug resistance and contributes to the resilience of the pathogen in infected hosts [10]. Membrane and exported proteins are crucial players for maintenance and survival of bacterial organisms, and their contribution to pathogenesis and immunological responses make these proteins relevant targets for medical research [11]. In particular, these proteins are known to play pivotal roles in host-pathogen interactions and, therefore, represent potential drug targets and vaccine candidates [12].

Overall, the bulk of exported proteins are transported by the general secretory Sec-translocase pathway. This is performed by recognition of the signal peptide in the nascent preprotein, which is subsequently transferred to the machinery that executes its translocation across the membrane [13]. Besides, mycobacteria utilize type VII secretion systems (T7SS) to export many of their important virulence proteins. The T7SS encompasses five homologous secretion systems (designated ESX-1 through ESX-5). Most pathogenic mycobacterial species, including the human pathogen *M. tuberculosis*, possess all five ESX systems [14,15]. The ability of MTB to subvert host immune defenses is related to the secretion of multiple virulence factors via these specialized secretion systems [15].

Recent developments in mass spectrometry-based proteomics have highlighted the occurrence of numerous types of post-translational modifications (PTMs) in proteomes of prokaryotes which create an enormous diversity and complexity of gene products [16]. This PTMs, mainly

93 glycosylation, lipidation and phosphorylation, are involved in signaling and response to stress,
94 adaptation to changing environments, regulation of toxic and damaged proteins, protein
95 localization and host-pathogen interactions. In MTB, more frequently O-glycosylation events
96 have been reported [17], being this post-translational modification often found, in conjunction
97 with acylation, in membrane lipoproteins [18]. A mechanistic model of this modification was
98 proposed in which the initial glycosyl molecule is transferred to the hydroxyl oxygen of the
99 acceptor Thr or Ser residue, a process catalyzed by the protein O-mannosyltransferase (PMT)
100 (Rv1002c) [19]. Hereafter, further sugars are added one at a time, but the enzymes involved in
101 this elongation are still unknown [16]. O-glycosylation appears essential for MTB virulence, since
102 Rv1002c deficient strains are highly attenuated in immunocompromised mice [20]. Despite the
103 vital importance of glycosylated proteins in MTB pathogenesis, the current knowledge in this
104 regard is still limited. Recent evidence using whole cell extracts revealed that glycosylation could
105 be much more frequent than previously thought, explaining the phenotypic diversity and
106 virulence in the *Mycobacterium tuberculosis* complex [17], but in culture filtrates of this
107 pathogen only a few secreted and cell wall-associated glycoproteins have been described to date
108 [18,21].
109 In this study we describe a straightforward methodology based on a high throughput label-free
110 quantitative proteomic approach in order to provide a comprehensive identification and
111 quantitation of proteins in *M. tuberculosis* H37Rv culture filtrate. The extent of protein O-
112 glycosylation was also evaluated with the purpose of collaborating with the glycoproteomic
113 characterization of this pathogen. With the goal to validate and integrate our results, a
114 comprehensive comparative analysis was performed against former research papers that have
115 addressed this issue using different and complementary approaches. The results presented here
116 make focus on the principal exported and secreted virulent factors with the aim to contribute
117 to a deep proteomic characterization of this relevant pathogen and to collaborate to a better
118 understanding of the pathogenesis and survival strategies adopted by MTB.

Materials and Methods

Mycobacterial strain and growth conditions

Mycobacterium tuberculosis H37Rv strain (ATCC® 25618™) was grown for 3 weeks at 37°C in Lowenstein Jensen solid medium and after growth was achieved it was subcultured in Middlebrook 7H9 broth supplemented with albumin, dextrose, and catalase (ADC) enrichment (Difco, Detroit, MI, USA) for 12 days with gentle agitation at 37°C. Mycobacterial cells were pelleted at 4000xg for 15 min at 4°C and washed 3 times with cold phosphate-buffered saline. Mycobacterial cells were subsequently cultured as surface pellicles for 3 to 4 weeks at 37°C without shaking in 250 mL of Sauton minimal medium, a synthetic protein-free culture medium, which was prepared as previously described [8].

Culture filtrate protein preparation

Bacterial cells were removed by centrifugation and culture filtrate protein (CFP) was prepared by filtering the supernatant through 0.2 µM pore size filters (Millipore, USA). After sterility testing of CFP in Mycobacteria Growth Indicator Tube (MGIT) supplemented with MGIT 960 supplement (BD, Bactec) for 42 days at 37°C in BD BACTEC™ MGIT™ automated mycobacterial detection system, CFP was concentrated using centrifugal filter devices (Macrosep Advance, 3kDa MWCO (Pall Corporation, USA)). Concentrated CFP was buffer exchanged to phosphate-buffered saline and total protein concentration was quantified by BCA (Pierce BCA Protein Assay Kit, Thermo Fischer Scientific).

1D and 2D gel electrophoresis

M. tuberculosis CFP samples were analyzed by 1D and 2D gel electrophoresis and were used for raising polyclonal antibodies in rabbits as described below. For 1D gel electrophoresis CFP diluted in SDS-PAGE loading buffer was loaded onto 15% SDS-PAGE and silver nitrate staining

was performed as described elsewhere [22]. For 2-Dimensional gel electrophoresis 50 µg of *M. tuberculosis* CFP was purified and concentrated using 2-D Clean-Up Kit (GE Healthcare) and resuspended in 125 µl of rehydration solution (urea 7M, thiourea 2M, CHAPS 2%, IPG Buffer 3-10 0,5%, DTT 20 mM, bromophenol blue 0,002%). Two experiments were run in parallel, one for silver nitrate staining and the other for western blot analysis. Proteins were loaded into 7 cm IPG Strips 3-10 (GE Healthcare) by overnight passive rehydration. First dimension isoelectric focusing (IEF) run was performed using Ettan IPGphor 3 IEF System (GE Healthcare) according to manufacturer instructions. Disulfide bonds were reduced with dithiothreitol (10 mg/mL) and subsequently alkylated with 25 mg/mL iodoacetamide. The second dimension was performed on hand-cast gels (15% SDS-PAGE, 10x10x0.1cm) and silver nitrate staining was performed as described above. In both analyses the molecular weight marker was PageRuler Prestained Protein Ladder (Thermo Fischer Scientific). For Western blot analysis, proteins were transferred onto a nitrocellulose membrane (Amersham Protran 0.45 µM NC (GE Healthcare)) for one hour at 400mA. Membrane was blocked and blotted as described below.

Anti-CFP antibodies production and western blot

To produce polyclonal antibodies against *M. tuberculosis* CFP, two New Zealand White rabbits (2-2.5 kg) were immunized subcutaneously with 100 µg of CFP, followed by 1 booster of 100 µg and 2 additional boosters (50 µg each) of CFP in Incomplete Freund Adjuvant using an authorized protocol (Comité de Etica de Facultad de Química, Exp. Nº 101900-000717-14). At the end the rabbits were bled and a pool of hyperimmune serum was obtained as described elsewhere [23]. Anti-CFP polyclonal antibodies were purified by affinity chromatography using a HiTrap Protein A HP column (GE Healthcare) according to manufacturer instructions.

Anti-CFP polyclonal antibodies were used to identify immunoreactive bands and spots in 1D and 2D electrophoresis. Briefly, blocked membranes were incubated for 1h at room temperature with anti-CFP antibodies at a final concentration of 10 µg/mL in PBS pH7.4, 5% low fat milk. For

antigen-antibody detection membranes were incubated for 1h at room temperature with a 1:2500 dilution of anti-rabbit IgG (whole molecule)— alkaline phosphatase antibody produced in goat (Sigma A0545) in PBS pH7.4, 5% low fat milk. Membranes were incubated with SuperSignal™ West Pico PLUS Chemiluminescent Substrate (Thermo Fischer Scientific, #34580) according to manufacturer instructions. Images were acquired with Synoptics 4.2MP Camara using increasing and accumulative exposure times in G:Box Chemi XT4 (Syngene, Cambridge, UK) and visualized with GenSys Software (V1.3.3.0). The following reagent, obtained through BEI Resources, NIAID, NIH: Polyclonal Anti-Mycobacterium tuberculosis CFP minus LAM (antiserum, Rabbit), NR-13809, was used to confirm the immune recognition of our Anti-CFP polyclonal antibody. Some of the protein spots recognized by the anti-CFP antibody were further analyzed by mass spectrometry (MS).

Protein identification by MALDI-TOF/TOF.

Bands or spots from 1D or 2D gel electrophoresis were selected for MS MALDI-TOF/TOF analysis. In-gel Cys alkylation was performed by subsequent incubation with 10 mM dithiothreitol and 55 mM iodoacetamide as previously described [24]. In-gel digestion of selected protein bands or spots was performed overnight at 37 °C by incubation with trypsin (Sequencing grade, Promega, Madison, USA). Afterwards peptides were extracted as previously described [24] and samples were vacuum-dried using CentriVap Vacuum Concentrator (Labconco), resuspended in 0.1% TFA, and desalted using C18 OMIX tips (Agilent). Peptides were eluted with matrix solution (α-cyano-4-hydroxycinnamic acid in 60% acetonitrile, 0.1% TFA) directly into the MALDI sample plate. Spectra acquisition was performed on a 4800 MALDI TOF/TOF (Abi Sciex) operating in positive reflector mode. Spectra were externally calibrated using a mixture of peptide standards (Applied Biosystems).

MS/MS analysis of selected precursor ions was performed. Database searching (NCBInr 20150912) was performed with Mascot (http://www.matrixscience.com) using the following

parameters: unrestricted taxonomy; one trypsin missed cleavage allowed; methionine oxidation and carbamidomethylation of cysteine as variable modification; peptide tolerance of 0.05 Da and a MS/MS tolerance of 0.4 Da. Significant protein scores ($p < 0.05$) and at least one peptide with significant ions score ($p < 0.05$) per protein were used as criteria for positive identification [25].

Liquid chromatography tandem mass spectrometry (LC MS/MS)

Two replicas of *M. tuberculosis* CFP (25 μg) were loaded in SDS-PAGE 15% and stained with CCB G-250 as described elsewhere [26]. Six gel slices were excised from each lane according to protein density. In-gel Cys alkylation, in gel-digestion and peptide extraction was performed as described above. Tryptic peptides were separated using nano-HPLC (UltiMate 3000, Thermo Scientific) coupled online with a Q-Exactive Plus hybrid quadrupole-Orbitrap mass spectrometer (Thermo Fischer Scientific). Peptide mixtures were injected into a trap column Acclaim PepMap 100, C18, 75 um ID, 20 mm length, 3 um particle size (Thermo Scientific) and separated into a Reprosil-Pur 120 C18-AQ, 3 μm (Dr. Maisch) self-packed column (75μm ID, 49 cm length) at a flow rate of 250 nL/min. Peptide elution was achieved with 105 min gradient from 5% to 55% of mobile phase B (A: 0.1% formic acid; B: 0.1% formic acid in 80% acetonitrile). The mass spectrometer was operated in data-dependent acquisition mode with automatic switching between MS and MS/MS scans. The full MS scans were acquired at 70K resolution with automatic gain control (AGC) target of 1×10^6 ions between m/z = 200 to 2000 and were surveyed for a maximum injection time of 100 milliseconds (ms). Higher-energy collision dissociation (HCD) was used for peptide fragmentation at normalized collision energy set to 30. The MS/MS scans were performed using a data-dependent top12 method at a resolution of 17.5K with an AGC of 1×10^5 ions at a maximum injection time of 50 ms and isolation window of 2.0 m/z units. A dynamic exclusion list with a dynamic exclusion duration of 45 s was applied.

LC-MS/MS data analysis

LC-MS/MS data analysis was performed in accordance to the PatternLab for proteomics 4.0 software (http://www.patternlabforproteomics.org) data analysis protocol [27].The proteome (n=3993 proteins) from *M. tuberculosis* (Reference strain ATCC 25618/H37Rv UP000001584) was downloaded from Uniprot (March 2017) (https://www.uniprot.org/proteomes/). A target-reverse data-base including the 123 most common contaminants was generated using PatternLab's database generation tool. Thermo raw files were searched against the database using the integrated Comet [28] search engine (2016.01rev.3) with the following parameters: mass tolerance from the measured precursor m/z(ppm): 40; enzyme: trypsin, enzyme specificity: semi-specific, missed cleavages: 2; variable modifications: methionine oxidation; fixed modifications: carbamidomethylation of cysteine. Peptide spectrum matches were then filtered using PatternLab's Search Engine Processor (SEPro) module to achieve a list of identifications with less than 1% of false discovery rate (FDR) at the protein level [29]. Results were post-processed to only accept peptides with six or more residues and proteins with at least two different peptide spectrum matches. These last filters led to an FDR at the protein level, to be lower than 1% for all search results. Proteins were further grouped according to a maximum parsimony criteria in order to identify protein clusters with shared peptides and to derive the minimal list of proteins [30]. Spectrum counts of proteins identified in each technical replicate were statistically compared with unpaired Mann-Whitney test.

For the O-glycosylation analysis raw files were searched against the same database using the parameters described above with the addition of the following variable modifications in S or T amino acid residues: Hex =162.052824 Da, Hex-Hex=324.1056 Da, Hex-Hex-Hex=486.1584 Da, Pentose=132.042259 Da, Heptose=192.0633 Da, DeoxyHex=146.0579 Da. Monoisotopic mass of each neutral loss modification was defined in Comet search engine according to the values recorded in Unimod public domain database (http://www.unimod.org/). Each O-glycosylation was tested independently and a maximum of 2 modifications per peptide was allowed.

Peptide spectrum matches were filtered and post-processed using SEPro module, using the same parameters as described above and proteins were grouped according to a maximum parsimony criteria [30].

Protein analysis

Identified proteins in each replicate were compared by area-proportional Venn Diagram comparison (BioVenn [31]) and a list of common proteins was generated. Further analysis only considered proteins present in both replicates of LC MS/MS analysis. SEPro module retrieved a list of protein identified with Uniprot code. Molecular weight, length, complete sequence, gene name and *M. tuberculosis* locus identified (Rv) was obtained using the Retrieve/ID mapping Tool of Uniprot website (https://www.uniprot.org/uploadlists/) [32]. Protein functional category was obtained by downloading *M. tuberculosis* H37Rv genome sequence Release 3 (2018-06-05) from Mycobrowser website (https://mycobrowser.epfl.ch/) [33].

Protein O-glycosylation analysis

Proteins bearing O-glycosylated peptides in both replicates were compared by area-proportional Venn Diagram comparison (BioVenn [31]) and a list of common glycosylated proteins for each of the analyzed modifications, i.e. Hex, Hex-Hex, Hex-Hex-Hex, Pentose, Heptose, DeoxyHex, was generated. Further analysis was manually performed in order to identify common modified peptides in the list of common glycosylated proteins, as well as common modifications (as 1 peptide could contain up to two modifications). As a result of this analysis a list of proteins with common modifications was generated, consisting in proteins having the same modified peptide in both replicates. This list of O-glycosylated proteins was considered for subsequent analysis.

Signal peptide prediction

In order to identify potentially secreted proteins, the SignalP 5.0 Server (http://www.cbs.dtu.dk/services/SignalP/) was used to detect the presence of N-terminal signal sequences in the analyzed set of proteins. The organism group selected was gram-positive bacteria. This version of the Server, recently launched, can predict proteome-wide signal peptides across all organisms, and classify them into three type of signal peptides: Sec/SPI (SP), Sec/SPII (LIPO) and Tat/SPI (TAT) [34]. In the output produced by the server one annotation is attributed to each protein, the one that has the highest probability. The protein can have a Sec signal peptide (Sec/SPI), a Lipoprotein signal peptide (Sec/SPII), a Tat signal peptide (Tat/SPI) or No signal peptide at all (Other). If a signal peptide is predicted, the cleavage site (CS) position is also reported.

Estimation of protein abundance and comparative analysis

To estimate protein abundance Normalized Spectral Abundance Factor (NSAF) calculated with PatternLab for proteomics software was considered. NSAF allows for the estimation of protein abundance by dividing the sum of spectral counts for each identified protein by its length, thus determining the spectral abundance factor (SAF), and normalizing this value against the sum of the total protein SAFs in the sample [35,36]. Proteins were ordered according to their NSAF, from more to less abundant. NSAF values corresponding to percentile 75th, 90th and 95th were calculated, and the groups of proteins above these values were identified as $P_{75\%}$, $P_{90\%}$ and $P_{95\%}$ proteins, respectively. The list of proteins obtained in this study was compared with other proteomic studies [7,13,37] by Venn Diagram comparison (Venny 2.1, BioinfoGP [38]) and NSAF of proteins identified in all studies, 3 studies, 2 studies or only this study were statistically compared with unpaired Mann-Whitney test. The protein abundance determined for CFP identified in this study (NSAF) was compared with the protein abundance calculated for *M.*

tuberculosis proteins identified in a previous study using the exponentially modified protein abundance index (emPAI) [13].

Protein classification

Gene Onthology (GO) analysis of the culture filtrate proteins was performed with David Gene Functional Classification Tool [39,40] using the Cellular Component Ontology database and *M. tuberculosis* H37Rv total proteins as background. With this analysis principal categories of enriched terms ($p<0.05$) for $P_{75\%}$, $P_{90\%}$, $P_{95\%}$ and total proteins were determined. Functional classification of culture filtrate proteins was performed according to functional categories of *M. tuberculosis* knowledge database (Mycobrowser [33]).

Proteins with O-glycosylation modifications were analyzed with David Gene Functional Classification Tool [39,40] using Cellular Component, Biological Processes and Molecular functions Ontology database and *M. tuberculosis* H37Rv total proteins as background.

O-glycosylation validation

The same analytical workflow described previously for LC-MS/MS analysis of O-glycosylation in our data was performed using the raw data files deposited at the ProteomeXchange Consortium with the dataset identifier PXD000111 [37]. This analysis was performed in order to validate the modified peptides identified in our work against additional biological replicates obtained in a previous work that extensively characterized culture filtrate proteins of *M. tuberculosis* H37Rv [37]. Additionally, some relevant scans corresponding to glycosylated peptides were searched in Mascot Server MS/MS Ions Search (Mascot, Matrix Science Limited [41]). Search was performed against NCBIprot (AA) database of all taxonomies. Search parameters were defined as peptide mass tolerance: ± 10 ppm, MS/MS mass tolerance: ± 0.15 Da, enzyme: semiTrypsin, fixed modifications: Carbamidomethyl (C), variable modifications: Hex (ST), Hex(2) (ST), Hex(3) (ST), Pent (ST), Hept (ST) or dHex (ST), according to the searched peptide. Other parameters were set to default values.

Results and Discussion

M. tuberculosis culture filtrate proteins quality evaluation

M. tuberculosis H37Rv was cultured following a classical method using Sauton minimal medium, a synthetic protein-free culture medium compatible with proteomic downstream analysis [8]. Culture filtrate proteins (CFP), obtained after culture centrifugation and filtration, were concentrated by ultrafiltration and quantitated previous to further analysis. Four different batches of CPF were analyzed by gel electrophoresis and silver nitrate staining. As similar patterns were observed with the different CFP preparations a composed sample was prepared. The composed CFP sample was separated and resolved by 1D and 2D gel electrophoresis. In 1D SDS-PAGE an electrophoretic pattern showing a variety of proteins from approx. 10 kDa to 100 kDa was observed (Fig 1A). In the case of 2D gel electrophoresis analysis, two experiments were run in parallel, one for silver nitrate staining (Fig 1B) and the other for western blot analysis using anti-CFP rabbit polyclonal antibodies to identify principal immunogenic proteins (Fig 1C). Immune recognition pattern of CFP proteins observed with anti-CFP rabbit polyclonal antibody was confirmed with an additional anti-CFP polyclonal antibody (NR-13809, BEI Resources).

Fig 1. Analysis of *M. tuberculosis* CFP by electrophoresis and *western blot*.

(A) *M. tuberculosis* CFP analysis by 1D SDS-PAGE 15% and silver nitrate staining. Two different batches (lanes 1 and 2, 1.8 and 2.1 ug, respectively) and a composed and concentrated sample of both batches (lane 3, 12 ug) were loaded. Bands selected for MALDI-TOF/TOF mass spectrometry are indicated as H1, H2, H3 and H4. MWM: Molecular weight marker (Thermo Fischer Scientific, # 26616). (B) *M. tuberculosis* CFP analysis by 2D electrophoresis and silver nitrate staining. *M. tuberculosis* CFP composed sample (50 ug) was loaded. Immunoreactive spots selected for MALDI-TOF/TOF mass spectrometry are indicated with numbers. MWM: Molecular weight marker (Thermo Fischer Scientific, # 26616). (C) Western blot analysis of *M. tuberculosis* CPF. 2D gel performed equally as (B) was transferred to Protran 0.45 uM NC (GE

Healtcare) and probed with rabbit anti-CFP antibody. Immunoreactive zones are indicated with a rectangle in the corresponding 2D gel.

As shown in Fig 1B most of the spots consisted of proteins with an isoelectric point below 6.5, as was previously reported by others [7,8,42,43]. Some immunoreactive spots detected in 2D western blot were overlapped with 2D gel silver nitrate stained to select candidates to be analyzed by mass spectrometry (Fig 1C). By this MS analysis 12 different proteins of *M. tuberculosis* (MTB) were identified in the CFP sample (Table 1) as well as some low-signal contaminant keratin peptides. Molecular weight of identified MTB proteins showed a good correlation with the relative molecular weight of selected band or spot (Table 1).

Table 1. *M. tuberculosis* proteins identified by MALDI-TOF (MS/MS) from 1D and 2D SDS polyacrylamide electrophoresis.

Band / spot	Protein	Molecular weight	Gene name	Gene identifier	Proteomics	Functional category
H1	Conserved protein with FHA domain, GarA	17,2 kDa	*garA*	**Rv1827**	CF, CYT, CW, MF.	Conserved hypothetical
H1	Adenylate kinase Adk (ATP-AMP transphosphorylase)	20,0 kDa	*adk*	**Rv0733**	CF, CYT, MF.	Intermediary metabolism and respiration
H1	Superoxide dismutase [FE] SodA	23,0 kDa	*sodA*	**Rv3846**	CF, CYT, MF.	Virulence, detoxification, adaptation
H2	Conserved protein TB18.6	18,6 kDa	TB18.6	**Rv2140c**	CF, MF.	Conserved hypotheticals
H2	Probable thiol peroxidase Tpx	16,8 kDa	*tpx*	**Rv1932**	CF, CYT, MF.	Virulence, detoxification, adaptation
H3	10 kDa chaperonin GroES	10,8 kDa	*groES*	**Rv3418c**	CF, CYT, CW, MF.	Virulence, detoxification, adaptation
H3/1/2/6	Heat shock protein HspX (alpha-crystallin homolog)	16,2 kDa	*hspX*	**Rv2031c**	CF, CYT, CW, MF.	Virulence, detoxification, adaptation
H4/1/6	10 kDa culture filtrate antigen EsxB	10,8 kDa	*esXB*	**Rv3874**	CF, CYT, MF.	Cell wall and cell processes
1/2/3/4	ESAT-6 like protein (Identification could correspond to EsxJ, EsxK, EsxM, EsxP or EsxW)	≅ 10 kDa	*esxJ* *esxK* *esxM* *esxP* *esxW*	**Rv1038c** **Rv1197** **Rv1792** **Rv2347c** **Rv3620c**	CF*	Cell wall and cell processes
2	Thioredoxin TrxC (TRX) (MPT46)	12.5 kDa	*trxC*	**Rv3914**	CF, CYT, CW, MF.	Intermediary metabolism and respiration
5	Secreted antigen 85-a FbpA (mycolyl transferase 85A)	35.7 kDa	*fbpA*	**Rv3804c**	CF, CYT, CW, MF.	Lipid metabolism
6	Rv3747	13.5 kDa	Rv3747	**Rv3747**	MF	Conserved hypotheticals

CF: Culture filtrate, CYT: Cytosol, CW: Cell Wall, MF: Membrane fraction, * Putative (EsxK, EsxM), reported (EsxJ, EsxW), not reported (EsxP). Table filled with information obtained from Ref [33].

All proteins identified by this approach were previously detected in other proteomic studies, and most of them (11 out of 12) were identified in the culture filtrate fraction by at least one earlier proteomic report [33]. Besides, 3 proteins were identified in at least 3 different bands or spots, reflecting the fact that these proteins could be highly represented in CFP. These are heat shock protein HspX (Rv2031c), 10 kDa culture filtrate antigen EsxB (Rv3874) and a group of indistinguishable proteins (ESAT-6 like proteins). As proteins of this group - EsxJ (Rv1038c), EsxK (Rv1197), EsxM (Rv1792), EsxP (Rv2347c) and EsxW (Rv3620c) - are 98 amino acids long and

differ in only 1 or two amino acids, the unequivocal identification of each one is hindered. Proteins of ESAT-6 like group were identified in a common zone of the 2D gel (spots 1 to 4), suggesting that each spot could correspond to a slightly different protein isoform.

These results indicated that the *M. tuberculosis* H37Rv CFP preparation provides a good representation of the secreted/shed proteins because many main proteins of MTB were identified, with minimal contamination of non-MTB proteins (only a few peptides of human keratin were detected). Proteins highly recognized by anti-CFP antibodies (HspX, EsxB and Secreted antigen 85-a FbpA (Rv3804c)) are relevant pathogen antigens [33,44], recognized as secreted proteins by others [8,13], and evaluated as pathogen-derived biomarkers for active tuberculosis diagnosis [9].

Characterization of CFP using LC MS/MS

Although 2D gel electrophoresis coupled with MALDI TOF/TOF analysis is an extremely powerful tool to dissect and resolve multiprotein complexes, it is a low performance methodology for proteomic analysis, which needs a laborious and systematic approach in order to get confident and sensitive identification of proteins present in complex samples. Our results showed that this analysis generated several cases of redundant identifications. Thus, after quality confirmation of the sample, a high throughput analysis was performed using a shotgun quantitative approach based on a liquid nano-HPLC and tandem mass spectrometry workflow. In this experiment the proteins present in two technical replicates were resolved in SDS-PAGE and different portions of the gel were further selected for LC MS/MS analysis (S1A Fig). A gross initial quantitative comparison of spectrum counts of both datasets showed that there were not statistical differences among both replicates (S1B Fig). In CFP(1) 1450 different proteins were identified (corresponding 1427 to MTB, 19 to common contaminants and 4 to reverse sequences, resulting in a 0.28% FDR), whereas in CFP(2) 1453 different proteins were identified (1429 MTB proteins, 18 contaminants and 6 reverse sequences (0.41% FDR)). The list of proteins of each replica is

386 available in S1 Table. The mass spectrometry proteomics data (raw data and search files) have
387 been deposited at the MassIVE repository with the dataset DOI: doi:10.25345/C5PW8Q.
388 The qualitative comparison of both datasets using a Venn Diagram bioinformatic tool showed
389 that 1314 MTB proteins (92%) were shared between both replicates (S1C Fig). All proteins
390 previously identified in the CFP sample by gel electrophoresis and MALDI-TOF/TOF were
391 detected in both replicates characterized by LC MS/MS. The full list of 1314 common proteins,
392 which was used for further analysis, is provided in S1 Table. Proteins showed a wide distribution
393 of molecular weights, however most of them were of low molecular weight (median 31.97 kDa,
394 Q1 21.25 kDa, Q3 46.50 kDa), which was consistent with the profile observed in Fig 1A and 1B.
395 Previous research has shown that the vast majority of protein spots resolved in 2D gel
396 electrophoresis of *M. tuberculosis* H37Rv CFP were found in the molecular weight range of 6–70
397 kDa [8]. Moreover, consistent with our results, proteins identified by LC-MS/MS in a well
398 characterized CFP, showed that the majority of the proteins were found in the 10-50 kDa range,
399 with an average theoretical mass of 31.0 kDa [7].

400 ## Protein classification using a quali-quantitative analysis

401 Quantitative proteomics based on spectral counting methods are straightforward to employ and
402 have been shown to correctly detect differences between samples [45]. In order to consider
403 sample-to-sample variation obtained when carrying out replicate analyses, and due to the fact
404 that longer proteins tend to have more peptide identifications than shorter proteins, Patternlab
405 for Proteomics software uses NSAF (Normalized spectral abundance factor) [46] for spectral
406 counting normalization. The NSAF for a protein is the number of spectral counts (SpC, the total
407 number of MS/MS spectra) identifying a protein, divided by the protein's length (L), divided by
408 the sum of SpC/L for all N proteins in the experiment. NSAF was shown to yield the most
409 reproducible counts across technical and biological replicates [35]. Using the sum of NSAF of
410 both replicates (Total NSAF, included in S1 Table) the common list of CFP was ordered according

411 to protein abundance and arbitrarily grouped in 4 subgroups (P95%, P90%, P75% and total CFP),
412 consisting of 66, 132, 329 and 1314 proteins, respectively. P95% comprised proteins above 95th
413 percentile NSAF, thus representing the most abundant proteins in the sample. P90% and P75%
414 comprised proteins above 90th and 75th percentile, respectively. These subgroups of proteins
415 were functionally classified using Gene Ontology, Cellular Component analysis, and principal
416 categories of enriched terms ($p<0.05$) were determined (Fig 2A). Considering the subgroup of
417 total CFP proteins 4 principal categories (cell wall, cytoplasm, extracellular region and plasma
418 membrane) were similarly enriched (fold change 1.5, 1.5, 1.2 and 1.1, respectively). However,
419 when considering the subgroups of more abundant proteins, the categories cell wall and
420 extracellular region showed a marked increase of fold enrichment with protein abundance,
421 achieving these categories in P95% subgroup a fold enrichment of 2.9 (p=8.3e-18) and 3.1
422 (p=2.0e-8), respectively. This tendency was not observed in cytoplasm and plasma membrane
423 categories.
424
425 **Figure 2. Quali-quantitative protein classification.**
426 (A) Fold change of principal categories of enriched terms ($p<0.05$) obtained analyzing common proteins
427 of both replicates with David Gene Functional Classification Tool [39,40] using the Cellular Component
428 Ontology database and *M. tuberculosis* H37Rv total proteins as background. Proteins were ordered
429 considering normalized spectral abundance factor (NSAF) and percentile 75th, 90th and 95th NSAF were
430 calculated. Fold change of the lists above each defined percentile (P75%, P90% and P95% proteins) analyzed
431 using the same approach is shown. (B) Functional categories of CFP according to *M. tuberculosis*
432 knowledge database (Mycobrowser [33]). Bars represent number of proteins corresponding to each
433 category (number is indicated above each bar, scale in left axe) and dots represent mean NSAF of proteins
434 in each category (scale is indicated in right axe).
435
436 The results presented showed that CFP proteins prepared in this work besides containing
437 extracellular and cell wall proteins also include some cytoplasmatic and membrane proteins.

438 This observation should be relativized considering the fact that many CFP were classified with
439 more than one ontology term, thus redundant information of cellular component could be
440 obtained. Particularly, 183 proteins were classified as extracellular, but only 44 contained
441 exclusively this ontology term. Besides, only 125 proteins were classified as exclusively
442 cytoplasmatic, out of 463 proteins containing this ontology term. It is also important to note
443 that 394 proteins had no assigned GO term. Taken this into account the analysis performed
444 considering the abundance of each CFP protein in terms of NSAF could be more indicative of the
445 actual composition of the sample. In that regard, our analysis indicates that the subgroups of
446 more abundant proteins contained mainly proteins of extracellular region and cell wall
447 compartment.
448 The annotated *M. tuberculosis* H37Rv proteins have been classified into 12 distinct functional
449 categories in the *M. tuberculosis* knowledge database (Mycobrowser [33]). Functional
450 classification of proteins identified in this study according to this classification showed that
451 proteins were distributed across ten of those functional groups (Fig 2B). Most of the identified
452 proteins are involved in intermediary metabolism and respiration (35.9%). However, when
453 protein abundance is considered, the category with higher protein mean NSAF is virulence,
454 detoxification, adaptation followed by cell wall and cell processes (Fig 2B).
455 Finally, considering the need of pathogen-derived biomarker validation for *M. tuberculosis*
456 active diagnosis, we looked in the list of CFP for principal protein antigens detected in clinical
457 samples [9], confirming the presence of 11 out of 12. Moreover, these putative biomarkers
458 exhibited on average a high NSAF, being 10 of them in the P90% subgroup: GroEL2 (Rv0440), EsxA
459 (Rv3875), HspX (Rv2031c), FbpA (Rv3804c), FbpB (Rv1886c), Mpt64 (Rv1980c), PstS1 (Rv0934),
460 GlcB (Rv1837c), Apa (Rv1860) and FbpC (Rv0129c).

Prediction of secreted proteins

Given the results obtained the question arises whether the presence of certain proteins in CFP is due to bacterial leakage/autolysis in combination with high levels of protein expression and extracellular stability, rather than to protein-specific export mechanisms. *M. tuberculosis* H37Rv reference proteome (UP000001584) obtained from UniProt and our list of proteins from culture filtrate was submitted to SignalP 5.0 signal peptide prediction [34]. This method incorporates deep recurrent neural network-based approach that improves signal peptide (SP) prediction across all domains of life and distinguishes between three types of prokaryotic SPs, i.e., SP (Sec/SPI): standard secretory signal peptides transported by the Sec translocon and cleaved by Signal Peptidase I, Sec/SPII (LIPO): lipoprotein signal peptides transported by the Sec translocon and cleaved by Signal Peptidase II and Tat/SPI (twin-arginine translocation pathway, TAT): signal peptides transported by the Tat translocon and cleaved by Signal Peptidase I. A total of 392 proteins were predicted to have one of these types of signal peptide in *M. tuberculosis* proteome (207 SP, 113 LIPO and 72 TAT). Of those we identified 140 in CFP (62 SP, 53 LIPO and 25 TAT), being many of them well recognized secreted proteins, particularly FbpA (Rv3804c), FbpB (Rv1886c), FbpC (Rv0129c), Apa (Rv1860), Mpt64 (Rv1980c), PstS1 (Rv0934), LpqH (Rv3736), among others (S2 Table).

This approach allowed for the identification of proteins targeted to the signal-sequence-dependent secretory pathways. To export proteins across its unique cell wall, mycobacteria utilize the general secretion pathways, twin-arginine transporter, and up to five distinct ESX secretion systems (designated ESX-1 through ESX-5, referred to as the type VII secretion system: T7SS), which various functions in virulence, iron acquisition, and cell surface decoration [14]. The ESX-1 system was the first of the T7SS to be identified and is responsible for the secretion of EsxA (6 kDa early secretory antigenic target, ESAT-6, Rv3875) and EsxB (Rv3874) [47]. It is important to note that proteins belonging to ESX secretion systems gene clusters as well as closely related PE and PPE gene families are *M. tuberculosis* secreted proteins that do not have

487 classical secretion signals [15,48]. Taken this into consideration, we identified in CFP several
488 proteins of ESAT-6 family: EsxA (Rv3875), EsxB (Rv3874), EsxG (Rv0287), EsxI (Rv1037c), EsxK
489 (Rv1197) grouped with EsxP (Rv2347c) and EsxJ (Rv1038c), EsxL (Rv1198), EsxN (Rv1793)
490 grouped with EsxV (Rv3619c), EsxO (Rv2346c) and EsxW (Rv3620c). None of those were
491 predicted by SignalP to contain a signal peptide. Besides, various proteins of ESX-1 secretion
492 system detected in this analysis were not predicted to have a signal peptide, including EspA
493 (Rv3616c), EspD (Rv3614c), EspC (Rv3615c) and EspB (Rv3881c). All of them count with
494 experimental evidence of being secreted [32]. Finally, we detected 8 PE and PPE family proteins
495 in our sample, from which 3 were predicted to have a signal peptide, i.e., PE13 (Rv1195), PE5
496 (Rv0285) and PE15 (Rv1386) and 5 were not predicted to have a signal peptide, i.e., PE25
497 (Rv2431c), PE31 (Rv3477), PPE41 (Rv2430c), PPE18 (Rv1196) and PPE60 (Rv3478). In particular,
498 PE25 and PPE41 form a heterodimer that is secreted by the ESX-5 system of *M. tuberculosis* [49].
499 In summary, various proteins with signal peptides were detected in our sample and several other
500 proteins related to T7SS were identified. The SignalP 5.0 server was a suitable approach in order
501 to predict secreted proteins with classical signal peptides but it has limitations to analyze
502 proteins bearing non-classical secretion signals.

503 Integrative analysis with previous proteomic studies

504 In order to get more information on the results obtained and validate them, former research
505 studies, which used different and complementary approaches to characterize *M. tuberculosis*
506 *H37Rv* CFP, were compared against our results. We selected relevant previous proteomic studies
507 reporting a similar methodology of mycobacterial culture and CFP preparation [7,13,37]. Malen
508 *et al.* characterized a culture filtrate of *M. tuberculosis* H37Rv, considerably enriched for
509 secreted proteins, with two complementary approaches (i) 2D gel electrophoresis combined
510 with MALDI-TOF MS and (ii) LC coupled MS/MS. Peptides derived from a total of 257 proteins
511 were identified, of which 254 were annotated with an Rv identifier [7]. Later, de Souza *et al.*

using nano-LC in tandem with an Orbitrap mass spectrometer performed a proteomic screening to identify proteins in culture filtrate, membrane fraction and whole cell lysate of *Mycobacterium tuberculosis*. Through this approach they identified 2182 different proteins in the different fractions, specifically 458 proteins in CFP, 1447 in the membrane fraction and 1880 in the whole cell lysate [13]. In a recent report, Albrethsen *et al*. used label-free LC-MS/MS of SDS-PAGE fractionated samples to investigate the culture filtrate proteome of *M. tuberculosis* H37Rv bacteria in normal log-phase growth and after 6 weeks of nutrient starvation. In total, in this study 1362 proteins were identified in six CFP samples analyzed (three log phase samples and three 6-week-starved CFP samples) [37]. The comparison of proteins identified in our analysis against the proteins identified in CFP of these former proteomic researches showed a common group of 122 proteins consistently detected (Fig 3A). Among these proteins, 41 belong to the P90% subgroup indicating that these are highly abundant proteins. The most important proteins of this common group include 10 kDa chaperonin GroES (Rv3418c), ESAT-6-like protein EsxB (Rv3874), 6 kDa early secretory antigenic EsxA (Rv3875), Chaperone protein DnaK (Rv0350), the secreted antigen 85 complex -85A (Rv3804c), 85B (Rv1886c) and 85C (Rv0129c)-, Glutamine synthetase GlnA1 (Rv2220), Immunogenic protein Mpt64 (Rv1980c), Superoxide dismutase SodA (Rv3846), Thioredoxin TrxA (Rv3914), Glycogen accumulation regulator GarA (Rv1827), Phosphate-binding protein PstS1 (Rv0934), Alanine and proline-rich secreted protein Apa (Rv1860) and various other ESAT-6 family proteins (EsxO Rv2346c, EsxL Rv1198, EsxG Rv0287). Moreover, 1073 proteins were shared between our set of proteins and the list reported by Albrethsen *et al.* [37], representing 81.7% of the proteins identified by us and confirming a strong concordance between both analysis.

The label free quantitative approach applied in this study was exploited to compare the abundance in our sample of proteins identified in all the studies included in the analysis (N=4) versus those proteins identified in 3 (N=3), 2 (N=2) or 1 study (only this study) (N=1). Fig 3B clearly shows that proteins identified in the four studies are on average more abundant than

538 proteins identified in the other groups analyzed. Moreover, proteins identified in at least 2
539 studies (N=3 or N=2) are globally more abundant than proteins identified exclusively in the
540 present work.

541

542 **Fig 3. Comparison of *M. tuberculosis* CFP with other relevant proteomic studies.**
543 (A) Analysis of *M. tuberculosis* CFP protein list (CFP TB: this study) versus other relevant proteomic studies
544 of *M. tuberculosis* CPF, identified as CPF Malen [7], CFP de Souza [13] and CFP Albrethsen [37] by Venn
545 Diagram comparison (Venny's on-line reference [38]). (B) Protein abundance estimation of proteins
546 identified this study (CFP TB) and in all of the three other studies evaluated (N=4), in this study and in two
547 other studies (N=3), in this study and in one other study (N=2), or only in this study (N=1). The arrow
548 indicates the protein Rv3620c (esxW) that was identified in an additional study [8] not included in the
549 comparison of Fig 3A. The star indicates the protein Rv3118 (sseC1) which has an identical (100% identity)
550 second copy at Rv0814c (sseC2) which was identified in CFP Albrethsen [37]. p-value obtained after Mann-
551 Whitney test comparison of the median of two groups is shown, and the groups compared in each case is
552 indicated with a line above each graph.

553

554 Additional analysis comparing our data against the proteomic quantitative approach performed
555 by de Souza *et al* [13] allowed us to identify a subgroups of highly represented proteins
556 consisting of those identified in this work and also in the three fractions studied by this previous
557 work, i.e. culture filtrate, membrane fraction and whole cell lysate. This subgroup accounted for
558 43.2% of protein abundance expressed as NSAF in this work and 29.2% of emPAI calculated by
559 the cited research. Besides, a group of 921 proteins identified in membrane fraction and/or
560 whole cell lysate prepared by de Souza *et al* and accounting for 13.3 % of calculated emPAI was
561 not detected in the culture filtrate prepared by them neither in CFP prepared in this study [13].
562 These results are summarized in S3 Table.
563 As a whole these results show that the CFP prepared in the present work exhibited a good
564 correlation with previous studies, both in terms of qualitative proteomic composition as well as

565 in relation to the quantitative estimation of protein abundance. Proteins highly represented in
566 our sample are proteins either frequently identified by others using complementary approaches
567 in culture filtrates of MTB, and thus confirming that our sample is enriched in proteins that the
568 bacteria does secrete, or ubiquitously detected in different *M. tuberculosis* cellular fractions,
569 indicating that these could represent highly expressed proteins.
570 Finally, with this approach 30 proteins not previously annotated with proteomic data in
571 Mycobrowser website (Release 3 (2018-06-05)) [33] were identified (S4 Table). This list,
572 principally composed by proteins classified as conserved hypotheticals, includes the ESX-3
573 secretion-associated protein EspG3 (Rv0289) identified with 4 unique peptides in CFP(1) and 5
574 unique peptides in CFP(2) and the Two component sensor histidine kinase DosT (Rv2027c)
575 identified with 2 unique peptides in each replicate. Further comparison of these proteins with
576 the results obtained in a proteome-wide scale approach based on SWATH mass spectrometry
577 [50] allow us the identification, to the best of our knowledge, of 8 proteins without previous
578 evidence of expression at the protein level. In S5 Table these proteins are listed as well as the
579 scans of their corresponding peptides.

580 O-glycosylation analysis

581 To complement our analysis, the presence of the most common naturally occurring glycan
582 residues in mycobacteria was analyzed: hexoses, like mannose, glucose or galactose, which are
583 highly reported in mycobacterial lipoproteins [18], deoxyhexoses, like fucose and rhamnose,
584 that are important components of the cell surface glycans [51], the pentose sugar arabinose also
585 reported in some glycoproteins [18] and as part of the mycolyl-arabinogalactan-peptidoglycan
586 of the cell wall [52], and heptoses, recognized to be transferred by heptosyltransferases using
587 ADP-heptose [53]. Our rationale was that the nano LC MS/MS technology used in this work, by
588 having more than four orders of magnitude intrascan dynamic range and a femtogram-level

589 sensitivity, would allow the direct identification of modified peptides, without previous affinity-
590 based strategies for glycosylated protein enrichment.
591 In each replica several O-glycosylation events were detected and after comparing them a
592 reduced subgroup of common peptides and proteins was defined and selected for further
593 analysis. O-glycosylation profile analysis revealed the presence of 154 common glycosylation
594 events in 135 common modified peptides in both replicas of MTB culture filtrate (Table 2). The
595 O-glycosylated common peptides were identified in 363 scans, consisting in at least 2 scans per
596 peptide (1 scan per replica) and a maximum of 8 scans in the case of Hex-Hex-Hex modification
597 of Alanine and proline rich secreted protein Apa (Rv1860) (S6 Table). The four studied
598 monosaccharide modifications (Hex, Pentose, DeoxyHex and Heptose) were highly similarly
599 represented in culture filtrate proteins, being Hex the most frequent modification (Table 2). In
600 many cases the unmodified peptide was identified along with the modified peptide, indicating
601 that glycosylated and unglycosylated proteins isoforms are present (S2 Fig), as was previously
602 reported for the conserved lipoprotein LprG [54].
603
604 **Table 2. O-glycosylation profile of *M. tuberculosis* culture filtrate proteins identified by LC**
605 **MS/MS**

Modification	Replica # 1				Replica #2				
	Modified Peptides (n)	Peptide FDR (%, n/N)	Modified Proteins (n)	Protein FDR (%, n/N)	Modified Peptides (n)	Peptide FDR (%, n/N)	Modified Proteins (n)	Protein FDR (%, n/N)	Comm modif protein
Hex	268	**0.15** (27/17879)	212	**0.94** (14/1494)	107	**0.13** (22/16603)	95	**0.99** (15/1509)	36
Hex-Hex	94	**0.13** (22/17513)	91	**0.95** (14/1467)	72	**0.15** (25/16614)	67	**0.99** (15/1511)	23
Hex-Hex-Hex	68	**0.14** (24/17635)	62	**1.00** (15/1505)	66	**0.12** (20/16716)	57	**0.99** (15/1515)	15
Pentose	280	**0.12** (22/17686)	239	**0.96** (14/1458)	128	**0.13** (21/16592)	116	**1.00** (15/1507)	39
Heptose	129	**0.15** (27/17507)	121	**0.94** (14/1485)	112	**0.15** (25/16566)	104	**1.00** (15/1504)	29
DeoxyHex	144	**0.13** (22/17587)	125	**0.94** (14/1493)	137	**0.16** (26/16638)	125	**0.99** (15/1513)	38

606 FDR: False discovery rate, n: number, N: total number.
607

608 O-glycosylation modification were detected in 108 different MTB culture filtrate proteins, 52 of
609 them presented at least 3 scans of the modified peptide and 12 bore more than one of the
610 searched modifications, i.e. Apa (Rv1860), EsxA (Rv3875), LpqH (Rv3763), LppO (Rv2290), CarB
611 (Rv1384), AceE (Rv2241), FhaA (Rv0020c), PstS1 (Rv0934), LprF (Rv1368), DsbF (Rv1677), Mpt64
612 (Rv1980c) and DevR (Rv3133c) (Fig 4A). What is Interesting to highlight is the high number of
613 scans of modified peptides corresponding to Apa (Rv1860), most of them corresponding to Hex,
614 Hex-Hex or Hex-Hex-Hex. This protein, also known as immunogenic protein MPT32 or 45-kDa
615 glycoprotein is a largely characterized secreted mannosylated glycoprotein [55] and in
616 agreement with previous reports we found scans corresponding to the presence of one, two or
617 three hexoses between T313, T315, T316 and T318 as glycosylation sites [21]. It is currently
618 believed that mannosylated proteins can act as potential adhesins and it was demonstrated that
619 Apa is associated with the cell wall and binds lung surfactant protein A (SP-A) and other immune
620 system C-TLs containing homologous functional domains [56]. The 19 kDa lipoprotein antigen
621 precursor LpqH (Rv3763), also showing an important number of Hex-Hex and Hex-Hex-Hex
622 modified peptides, is a well-known glycosylated protein exposed in the bacterial cell envelope,
623 that was postulated to be used by mycobacteria to enable their entry into the macrophage
624 through interaction with mannose receptors (MRs) of this host cells [57].
625
626 **Fig 4. Description of O-glycosylated proteins in *M. tuberculosis* CFP.**
627 (A) Scans of O-glycosylated peptides identified in MTB culture filtrate proteins. Each analyzed modification
628 is displayed with a different bar color. Individual scans of both replicates were considered and only 52
629 proteins identified by at least three different scans are shown in the graph. (B) Gene Ontology analysis of
630 MTB culture filtrate glycoproteins. Principal categories of enriched terms ($p<0.05$) obtained analyzing
631 proteins with common glycosylation in both replicates with David Gene Functional Classification Tool
632 [39,40] using Molecular Functions, Biological Processes and Cellular Component Ontology database and
633 *M. tuberculosis* H37Rv total proteins as background.
634

It is important to note that the precise O-glycosylation site assignation is hampered by the fact that collision energies used for peptide fragmentation cause the breakage of the weaker O-glycosydic bond leaving behind mostly unmodified fragments. Although the glycosylation site assignation was not the aim of our study, the utility XDScoring of Patternlab for proteomics developed for statistical phosphopeptide site localization [58], was preliminary tested in our data. Glycosylation site p-value is presented in S6 Table.

Glycosylation plays a significant role in MTB adaptive processes and in particular cell-cell recognition between the pathogen and its host is mediated in part by glycosylated proteins. Based on the Gene Ontology (GO) analysis of the glycoproteins identified, cellular response to starvation, protein folding and pathogenesis were highly enriched biological processes. Our GO analysis further showed that most of the glycoproteins identified were localized in the cell wall and extracellular region and that phosphopantetheine binding (including Mas, Pks2, PpsD, Pks13 and Pks5), 3-oxoacid CoA-transferase activity and oxygen sensor activity (DesV and DesR) were significantly enriched molecular function categories (Fig 4B).

O-glycosylation validation

Of the 108 identified glycoproteins 21 were identified as candidate glycoproteins in the lectin interacting enriched membrane protein using WGA-affinity capture [12]. Besides, 12 glycoproteins bearing mono- or polyhexose modifications in our analysis have been included in a recent review of protein glycosylation and lipoglycosylation in *M. tuberculosis* [18], where experimental evidence was summarized. Among them several lipoproteins are included: LprA (Rv1270c), LprF (Rv1368), LppO (Rv2290), LpqH (Rv3763), PstS1 (Rv0934) and Mpt83 (Rv2873). Moreover, four of these proteins were consistently found with the same type of hexose O-glycosylation in culture filtrate of MTB, i.e. Apa (Rv1860), LppO (Rv2290), Rv2799 and Rv3491 [21]. Our results confirm the presence of glycosylated lipoproteins in culture filtrate aiding to the growing evidence for glycosylation of mycobacterial lipoproteins [18,21]. Besides, we

identified mono- or polyhexose modifications in DsbF (Rv1677), a probable conserved lipoprotein. The same DsbF glycosylation pattern was reported in a recent glycoproteomic analysis of MTB cell lysates of four different linages [17]. In this work 27 proteins of our list were also described as O-glycosylated, including HtrA (Rv1223), Wag31 (Rv2145c), FbpB (Rv1886c) and Rv2411c.

To further evaluate the reproducibility of our results and validate them we looked for O-glycosylated proteins in the raw data files deposited by Albrethsen *et al*. [37] at the ProteomeXchange Consortium. By means of this approach 22 proteins with the same O-glycosylation type were found and after peptide sequence comparison we confirmed 20 modified peptides in common with our results, corresponding to 11 different proteins LprA (Rv1270c), DsbF (Rv1677), Rv1732c, Apa (Rv1860), AroE (Rv2552c), Rv2799, Mpt83 (Rv2873), SahH (Rv3248c), Rv3491, LpqH (Rv3763) and EsxA (Rv3875). The scans corresponding to these peptides are presented in S7 Table.

As a whole, we are reporting 62 novel O-glycosylated proteins including hexose, heptose, pentose or deoxyhexose, 10 of them being validated with raw data re-analysis of the selected previous work [37]. Several relevant scans corresponding to glycosylated peptides were statistically confirmed in Mascot Server MS/MS Ions Search against NCBIprot (AA) database of all taxonomies [41] (S3 Fig). Interestingly EsxA (Rv3875) was found with three different types of O-glycosylation - DeoxyHex, Pentose and Heptose – (Fig 4A). Of those the presence of two heptoses, one in T61 and the other in T63 was also identified in at least one replica of log phase culture filtrates in Albrethsen *et al*. [37] (S7 Table). A representative peptide spectrum of this modification including peptide ions fragment matches is shown in Fig 5. EsxA (Rv3875) and its chaperone protein EsxB (Rv3874), localized in Region of Difference 1 (RD1) of the MTB genome, are important virulence factors of MTB and the most immunodominant antigens thus far identified [59]. EsxA (or ESAT-6) is included in several vaccine candidates in development [60] and is also the core antigen in the IFN-γ release assays (IGRA) used to diagnose latent infection

686 [61]. A former report described that an N-terminal Thr acetylation (+42Da) was identified in
687 some species of this protein obtained in a short-term MTB culture filtrate [62] and other
688 literature mentioned this protein as being glycosylated [17,63], however, to our knowledge, we
689 are presenting novel evidence of several O-glycosylation events in this relevant secreted
690 antigen.

691

692 **Fig 5. EsxA heptose-modified peptide spectra**

693 (A) Representative spectrum of EsxA heptose-modified peptide statistically confirmed by Mascot Server
694 MS/MS Ions Search (HE = heptose). (B) Fragment ions matches indicated in bold red as reported in Mascot
695 Server.

696

697

Conclusion

Membrane and exported proteins are crucial players for maintenance and survival of bacterial organisms in infected hosts, and their contribution to pathogenesis and immunological responses make these proteins relevant targets for medical research [11]. Consistently, various of the proteins identified in *M. tuberculosis* CFP were proposed as relevant mycobacterial virulence factors [64], putative active infection biomarkers [9] or vaccine candidates [60,65].

This shotgun proteomic approach allowed a deep comprehension of *M. tuberculosis* H37Rv culture filtrate proteins reporting proteomic evidence in this sub-fraction for 1314 proteins. In that sense it is important to note that although this method is highly sensitive, specificity was prioritized by selecting as post-processing criteria that considered only proteins with at least two different peptide spectrum matches.

In addition to proteins that have not been previously reported in *M. tuberculosis* H37Rv CFP, we also found proteins consistently detected in previous proteomic studies which were further confirmed as highly abundant proteins. Many of these proteins were previously described in culture filtrates of MTB or detected in different *M. tuberculosis* cellular fractions, including membrane fraction and whole cell lysate. This could suggest that two complementary pathways are accounting for our observations. On one hand, the abundance of certain proteins in CFP appear to be truly related to protein-specific export mechanisms, while on the other hand the occurrence of some proteins in CFP due to bacterial autolysis in combination with high levels of protein expression and extracellular stability cannot be ruled out. Nevertheless, the GO ontology Cellular Component analysis and the integrative analysis performed with relevant research papers confirms that our sample is indeed enriched in proteins that the bacteria secretes to the extracellular space.

Supporting this, we could identify several proteins with predicted N-terminal signal peptide indicating that these are targeted to the secretory pathways [66], as well as various proteins

723 belonging to the ESX secretion systems, and PE and PPE families known to be secreted by T7SS,
724 but recognized as not to have classical secretion signals [48].
725 With the aim to assess the role of protein O-glycosylation in MTB virulence and host-pathogen
726 interactions [16,18], this study described the identification of 154 glycosylation events in 108
727 MTB proteins. In particular, several lipoproteins were found glycosylated in culture filtrate.
728 Lipoproteins have been shown to play key roles in adhesion to host cells, modulation of
729 inflammatory processes, and translocation of virulence factors into host cells [67]. The growing
730 evidence of glycosylation of mycobacterial lipoproteins including the results presented here,
731 indicates that glycosylation plays a significant role in the function and regulation of this group
732 of proteins. Along with lipoproteins, other relevant glycoproteins identified were mainly
733 involved in cellular response to starvation, protein folding and pathogenesis. As a novel
734 contribution of this work, we are reporting that the virulence factor EsxA is glycosylated in MTB
735 culture filtrate. It is important to note that in addition to EsxA other glycosylated proteins
736 identified in this work have been proposed as diagnostic biomarkers for TB active disease.
737 Protein glycosylation data presented here, including the coexistence of related protein
738 glycoforms evidenced in this work, should be considered for designing antibody-based
739 diagnostic test targeting *M. tuberculosis* antigens. Besides, as reported for other pathogens
740 [68,69], protein glycosylation diversity could be a key mechanism to provide antigenic variability
741 aiding in the immune subversion of this pathogen.
742 Our study provided an integrative evaluation of MTB culture filtrate proteins, bringing evidence
743 of the expression of some proteins not previously detected at protein level, and confirming and
744 enlarging the database of O-glycosylated proteins. This novel information may raise new
745 questions on the role of protein O-glycosylation on the biology of MTB, as well as it will
746 contribute to complement the knowledge of its relevant biomarkers, virulence factors and
747 vaccine candidates.
748

Acknowledgments

We thank Rosario Duran (IIBCE/ Institut Pasteur de Montevideo, Uruguay) for critical reading of the manuscript and helpful discussion about LC MS/MS experiment design and data analysis. We also thank Alejandro Leyva (Institut Pasteur de Montevideo, Uruguay) for technical assistance with Orbitrap mass spectrometer and Paulo C. Carvalho (Fiocruz, Brazil) for his valuable collaboration with data analysis in PatternLab for Proteomics. Finally, we would like to thank the staff of Comisión Honoraria de Lucha Antituberculosa y Enfermedades Prevalentes (Montevideo, Uruguay), for technical assistance with *M. tuberculosis* culture.

References

1. World Health Organization. Global Tuberculosis Report 2018. Geneva; 2018.
2. Meena LS, Rajni. Survival mechanisms of pathogenic Mycobacterium tuberculosis H37Rv. FEBS J. 2010 Jun;277(11):2416–27.
3. Ernst JD. Mechanisms of M. tuberculosis Immune Evasion as Challenges to TB Vaccine Design. Cell Host Microbe. 2018 Jul;24(1):34–42.
4. Chegou NN, Hoek KG, Kriel M, Warren RM, Victor TC, Walzl G. Tuberculosis assays: past, present and future. Expert Rev Anti Infect Ther. 2011 Apr 10;9(4):457–69.
5. Steingart KR, Flores LL, Dendukuri N, Schiller I, Laal S, Ramsay A, et al. Commercial serological tests for the diagnosis of active pulmonary and extrapulmonary tuberculosis: an updated systematic review and meta-analysis. PLoS Med. 2011;8(8):e1001062.
6. Verma R, Pinto SM, Patil AH, Advani J, Subba P, Kumar M, et al. Quantitative Proteomic and Phosphoproteomic Analysis of H37Ra and H37Rv Strains of Mycobacterium tuberculosis. J Proteome Res. 2017 Apr 7;16(4):1632–45.

773 7. Malen H, Berven FS, Fladmark KE, Wiker HG. Comprehensive analysis of exported
774 proteins from Mycobacterium tuberculosis H37Rv. Proteomics. 2007;7(10):1702–18.
775 8. Mattow J, Schaible UE, Schmidt F, Hagens K, Siejak F, Brestrich G, et al. Comparative
776 proteome analysis of culture supernatant proteins from virulent Mycobacterium
777 tuberculosis H37Rv and attenuated M. bovis BCG Copenhagen. Electrophoresis.
778 2003;24(19–20):3405–20.
779 9. Tucci P, González-Sapienza G, Marin M. Pathogen-derived biomarkers for active
780 tuberculosis diagnosis. Front Microbiol. 2014;5(OCT).
781 10. Niederweis M, Danilchanka O, Huff J, Hoffmann C, Engelhardt H. Mycobacterial outer
782 membranes: in search of proteins. Trends Microbiol. 2010 Mar;18(3):109–16.
783 11. Daffé M, Etienne G. The capsule of Mycobacterium tuberculosis and its implications for
784 pathogenicity. Tuber Lung Dis. 1999 Jun;79(3):153–69.
785 12. Bell C, Smith GT, Sweredoski MJ, Hess S. Characterization of the Mycobacterium
786 tuberculosis Proteome by Liquid Chromatography Mass Spectrometry-based
787 Proteomics Techniques: A Comprehensive Resource for Tuberculosis Research. J
788 Proteome Res. 2012 Jan 30;11(1):119–30.
789 13. de Souza GA, Leversen NA, Malen H, Wiker HG. Bacterial proteins with cleaved or
790 uncleaved signal peptides of the general secretory pathway. J Proteomics.
791 2011;75(2):502–10.
792 14. Solomonson M, Setiaputra D, Makepeace KAT, Lameignere E, Petrotchenko E V.,
793 Conrady DG, et al. Structure of EspB from the ESX-1 type VII secretion system and
794 insights into its export mechanism. Structure. 2015;23(3):571–83.
795 15. Shah S, Briken V. Modular Organization of the ESX-5 Secretion System in
796 Mycobacterium tuberculosis. Front Cell Infect Microbiol. 2016;6(May):1–7.
797 16. van Els CACM, Corbière V, Smits K, van Gaans-van den Brink JAM, Poelen MCM,
798 Mascart F, et al. Toward Understanding the Essence of Post-Translational Modifications

for the Mycobacterium tuberculosis Immunoproteome. Front Immunol. 2014;5:361.

17. Birhanu AG, Yimer SA, Kalayou S, Riaz T, Zegeye ED, Holm-Hansen C, et al. Ample glycosylation in membrane and cell envelope proteins may explain the phenotypic diversity and virulence in the Mycobacterium tuberculosis complex. Sci Rep. 2019 Dec 27;9(1):2927.

18. Mehaffy C, Belisle JT, Dobos KM. Mycobacteria and their sweet proteins: An overview of protein glycosylation and lipoglycosylation in M. tuberculosis. Tuberculosis. 2019;115:1–13.

19. VanderVen BC, Harder JD, Crick DC, Belisle JT. Export-mediated assembly of mycobacterial glycoproteins parallels eukaryotic pathways. Science (80-). 2005 Aug 5;309(5736):941–3.

20. Liu C-F, Tonini L, Malaga W, Beau M, Stella A, Bouyssie D, et al. Bacterial protein-O-mannosylating enzyme is crucial for virulence of Mycobacterium tuberculosis. Proc Natl Acad Sci. 2013 Apr 16;110(16):6560–5.

21. Smith GT, Sweredoski MJ, Hess S. O-linked glycosylation sites profiling in Mycobacterium tuberculosis culture filtrate proteins. J Proteomics. 2014 Jan 31;97:296–306.

22. Ausubel Brent R., Kingston R. E., Moore D. D., Seidman J. G., Smith J. A. and Struhl K. FM. Current protocols in molecular biology. John Wiley and Sons, New York.; 1999.

23. Howard GC, Kaser MR. Making and using antibodies : a practical handbook. Taylor & Francis/CRC Press; 2013.

24. Lima A, Duran R, Schujman GE, Marchissio MJ, Portela MM, Obal G, et al. Serine/threonine protein kinase PrkA of the human pathogen Listeria monocytogenes: biochemical characterization and identification of interacting partners through proteomic approaches. J Proteomics. 2011;74(9):1720–34.

25. Rossello J, Lima A, Gil M, Rodríguez Duarte J, Correa A, Carvalho PC, et al. The EAL-

domain protein FcsR regulates flagella, chemotaxis and type III secretion system in Pseudomonas aeruginosa by a phosphodiesterase independent mechanism. Sci Rep. 2017 Dec 31;7(1):10281.

26. Steinberg TH. Chapter 31 Protein Gel Staining Methods. In 2009. p. 541–63.

27. Carvalho PC, Lima DB, Leprevost F V, Santos MDM, Fischer JSG, Aquino PF, et al. PatternLab for proteomics 4.0: A one-stop shop for analyzing shotgun proteomic data. Nat Protoc. 2016 Jan 10;11(1):102–17.

28. Eng JK, Hoopmann MR, Jahan TA, Egertson JD, Noble WS, MacCoss MJ. A Deeper Look into Comet—Implementation and Features. J Am Soc Mass Spectrom. 2015 Nov 27;26(11):1865–74.

29. Carvalho PC, Fischer JSG, Xu T, Cociorva D, Balbuena TS, Valente RH, et al. Search engine processor: Filtering and organizing peptide spectrum matches. Proteomics. 2012 Apr 1;12(7):944–9.

30. Zhang B, Chambers MC, Tabb DL. Proteomic Parsimony through Bipartite Graph Analysis Improves Accuracy and Transparency. J Proteome Res. 2007 Sep;6(9):3549–57.

31. Hulsen T, de Vlieg J, Alkema W. BioVenn – a web application for the comparison and visualization of biological lists using area-proportional Venn diagrams. BMC Genomics. 2008 Oct 16;9(1):488.

32. UniProt Consortium T. UniProt: the universal protein knowledgebase. Nucleic Acids Res. 2018 Mar 16;46(5):2699–2699.

33. Kapopoulou A, Lew JM, Cole ST. The MycoBrowser portal: A comprehensive and manually annotated resource for mycobacterial genomes. Tuberculosis. 2011 Jan;91(1):8–13.

34. Almagro Armenteros JJ, Tsirigos KD, Sønderby CK, Petersen TN, Winther O, Brunak S, et al. SignalP 5.0 improves signal peptide predictions using deep neural networks. Nat Biotechnol. 2019 Feb 18;

851 35. McIlwain S, Mathews M, Bereman MS, Rubel EW, MacCoss MJ, Noble WS. Estimating
852 relative abundances of proteins from shotgun proteomics data. BMC Bioinformatics.
853 2012;13:308.
854 36. Sudha D, Kohansal-Nodehi M, Kovuri P, Manda SS, Neriyanuri S, Gopal L, et al.
855 Proteomic profiling of human intraschisis cavity fluid. Clin Proteomics. 2017;14(1):1–12.
856 37. Albrethsen J, Agner J, Piersma SR, Højrup P, Pham T V., Weldingh K, et al. Proteomic
857 Profiling of Mycobacterium tuberculosis Identifies Nutrient-starvation-responsive
858 Toxin–antitoxin Systems. Mol Cell Proteomics. 2013 May;12(5):1180–91.
859 38. Oliveros JC. Venny. An interactive tool for comparing lists with Venn's diagrams.
860 39. Huang DW, Sherman BT, Lempicki RA. Bioinformatics enrichment tools: paths toward
861 the comprehensive functional analysis of large gene lists. Nucleic Acids Res. 2009
862 Jan;37(1):1–13.
863 40. Huang DW, Sherman BT, Lempicki RA. Systematic and integrative analysis of large gene
864 lists using DAVID bioinformatics resources. Nat Protoc. 2009 Jan 1;4(1):44–57.
865 41. Perkins DN, Pappin DJC, Creasy DM, Cottrell JS. Probability-based protein identification
866 by searching sequence databases using mass spectrometry data. Electrophoresis. 1999
867 Dec 1;20(18):3551–67.
868 42. Proteome 2D-PAGE Database - Home [Internet]. [cited 2019 Jan 23]. Available from:
869 http://web.mpiib-berlin.mpg.de/cgi-bin/pdbs/2d-page/extern/index.cgi
870 43. Mattow J, Jungblut PR, Müller E-C, Kaufmann SHE. Identification of acidic, low
871 molecular mass proteins of Mycobacterium tuberculosis strain H37Rv by matrix-
872 assisted laser desorption/ionization and electrospray ionization mass spectrometry.
873 Proteomics. 2001 Apr;1(4):494–507.
874 44. Lew JM, Kapopoulou A, Jones LM, Cole ST. TubercuList - 10 years after. Tuberculosis
875 (Edinb). 2011;91(1):1–7.
876 45. Wang M, You J, Bemis KG, Tegeler TJ, Brown DPG. Label-free mass spectrometry-based

protein quantification technologies in proteomic analysis. Briefings Funct Genomics Proteomics. 2008 Jun 25;7(5):329–39.

46. Zybailov B, Mosley AL, Sardiu ME, Coleman MK, Florens L, Washburn MP. Statistical Analysis of Membrane Proteome Expression Changes in Saccharomyces cerevisiae. J Proteome Res. 2006 Sep;5(9):2339–47.

47. Stanley SA, Raghavan S, Hwang WW, Cox JS. Acute infection and macrophage subversion by Mycobacterium tuberculosis require a specialized secretion system. Proc Natl Acad Sci. 2003 Oct 28;100(22):13001–6.

48. Abdallah AM, Vandenbroucke-Grauls CMJE, Luirink J, Gey van Pittius NC, Cox J, Appelmelk BJ, et al. Type VII secretion — mycobacteria show the way. Nat Rev Microbiol. 2007;5(11):883–91.

49. Korotkova N, Freire D, Phan TH, Ummels R, Creekmore CC, Evans TJ, et al. Structure of the M ycobacterium tuberculosis type VII secretion system chaperone EspG 5 in complex with PE25-PPE41 dimer. Mol Microbiol. 2014;94(2):367–82.

50. Schubert OT, Ludwig C, Kogadeeva M, Zimmermann M, Rosenberger G, Gengenbacher M, et al. Absolute proteome composition and dynamics during dormancy and resuscitation of mycobacterium tuberculosis. Cell Host Microbe. 2015;18(1):96–108.

51. Maki M, Renkonen R. Biosynthesis of 6-deoxyhexose glycans in bacteria. Glycobiology. 2003 Dec 23;14(3):1R–15.

52. Alderwick LJ, Harrison J, Lloyd GS, Birch HL. The Mycobacterial Cell Wall--Peptidoglycan and Arabinogalactan. Cold Spring Harb Perspect Med. 2015 Mar 27;5(8):a021113.

53. Lu Q, Yao Q, Xu Y, Li L, Li S, Liu Y, et al. An Iron-Containing Dodecameric Heptosyltransferase Family Modifies Bacterial Autotransporters in Pathogenesis. Cell Host Microbe. 2014 Sep 10;16(3):351–63.

54. Alonso H, Parra J, Malaga W, Payros D, Liu C-F, Berrone C, et al. Protein O-mannosylation deficiency increases LprG-associated lipoarabinomannan release by

Mycobacterium tuberculosis and enhances the TLR2-associated inflammatory response. Sci Rep. 2017 Dec 11;7(1):7913.

55. Dobos KM, Khoo KH, Swiderek KM, Brennan PJ, Belisle JT. Definition of the full extent of glycosylation of the 45-kilodalton glycoprotein of Mycobacterium tuberculosis. J Bacteriol. 1996 May;178(9):2498–506.

56. Ragas A, Roussel L, Puzo G, Rivière M. The Mycobacterium tuberculosis Cell-surface Glycoprotein Apa as a Potential Adhesin to Colonize Target Cells via the Innate Immune System Pulmonary C-type Lectin Surfactant Protein A. J Biol Chem. 2007 Feb 23;282(8):5133–42.

57. Diaz-Silvestre H, Espinosa-Cueto P, Sanchez-Gonzalez A, Esparza-Ceron MA, Pereira-Suarez AL, Bernal-Fernandez G, et al. The 19-kDa antigen of Mycobacterium tuberculosis is a major adhesin that binds the mannose receptor of THP-1 monocytic cells and promotes phagocytosis of mycobacteria. Microb Pathog. 2005 Sep;39(3):97–107.

58. Fischer J de S d. G, dos Santos MDM, Marchini FK, Barbosa VC, Carvalho PC, Zanchin NIT. A scoring model for phosphopeptide site localization and its impact on the question of whether to use MSA. J Proteomics. 2014;129:42–50.

59. Lindestam Arlehamn CS, Sidney J, Henderson R, Greenbaum JA, James EA, Moutaftsi M, et al. Dissecting Mechanisms of Immunodominance to the Common Tuberculosis Antigens ESAT-6, CFP10, Rv2031c (hspX), Rv2654c (TB7.7), and Rv1038c (EsxJ). J Immunol. 2012 May 15;188(10):5020–31.

60. Khoshnood S, Heidary M, Haeili M, Drancourt M, Darban-Sarokhalil D, Nasiri MJ, et al. Novel vaccine candidates against Mycobacterium tuberculosis. Int J Biol Macromol. 2018 Dec;120:180–8.

61. Ruhwald M, de Thurah L, Kuchaka D, Zaher MR, Salman AM, Abdel-Ghaffar A-R, et al. Introducing the ESAT-6 free IGRA, a companion diagnostic for TB vaccines based on

ESAT-6. Sci Rep. 2017 May 7;7(1):45969.

62. Okkels LM, Müller EC, Schmid M, Rosenkrands I, Kaufmann SHE, Andersen P, et al. CFP10 discriminates between nonacetylated and acelylated ESAT-6 of Mycobacterium tuberculosis by differential interaction. Proteomics. 2004;4(10):2954–60.

63. Sonawane A, Mohanty S, Jagannathan L, Bekolay A, Banerjee S. Role of glycans and glycoproteins in disease development by Mycobacterium tuberculosis. Crit Rev Microbiol. 2012;38(3):250–66.

64. Forrellad MA, Klepp LI, Gioffré A, Sabio García J, Morbidoni HR, de la Paz Santangelo M, et al. Virulence factors of the Mycobacterium tuberculosis complex. Virulence. 2013;4(1):3–66.

65. Hatherill M, Tait D, McShane H. Clinical Testing of Tuberculosis Vaccine Candidates. In: Tuberculosis and the Tubercle Bacillus, Second Edition. American Society of Microbiology; 2016. p. 193–211.

66. Nielsen H. Predicting secretory proteins with signaIP. In: Methods in Molecular Biology. 2017. p. 59–73.

67. Kovacs-Simon A, Titball RW, Michell SL. Lipoproteins of Bacterial Pathogens. Infect Immun. 2011 Feb;79(2):548.

68. York IA, Stevens J, Alymova I V. Influenza virus N-linked glycosylation and innate immunity. Biosci Rep. 2019 Jan 31;39(1):BSR20171505.

69. Børud B, Bårnes GK, Brynildsrud OB, Fritzsønn E, Caugant DA. Genotypic and Phenotypic Characterization of the O-Linked Protein Glycosylation System Reveals High Glycan Diversity in Paired Meningococcal Carriage Isolates. J Bacteriol. 2018 Aug 15;200(16):e00794-17.

Supporting information

S1 Fig. Analysis of *M. tuberculosis* CFP by liquid chromatography tandem mass spectrometry (LC-MS/MS).

2A: *M. tuberculosis* CFP analysis by 1D SDS-PAGE 15% and CCB G-250 staining. Two technical replicates (CFP(1) and CFP(2), 25 ug each) were loaded. Six gel slices were excised from each lane according to protein density. Numbers indicate gel slices analyzed by LC-MS/MS. MWM: Molecular weight marker (Thermo Fischer Scientific, # 26616). **2B:** Spectrum counts of proteins identified in each technical replicate. Replicates show no statistical differences ($p>0.05$). **2C:** Analysis of proteins identified in each replicate by area-proportional Venn Diagram comparison [31]

S2 Fig. Proteins showing glycosylated and unglycosylated equivalent peptides.

Some protein examples are shown: 1) Apa (modification: Hex), 2) LprF (modification: Hex), LppO (modification: Hex-Hex), Apa (modification: Hex-Hex-Hex), EsxA (modification: Pentose).

S3 Fig. Scans of glycosylated peptides statistically confirmed in Mascot Server MS/MS Ions Search against NCBIprot (AA).

Some examples are shown: 1) LppO (modification: Hex), 2) EsxA (modification: DeoxyHex), 3) EsxA (modification: Pentose).

S1 Table. Proteins identified with nano-HPLC MS/MS.

Sheet 1) Common proteins list including Uniprot identification, protein description, protein length and molecular weight, gene name and *M. tuberculosis H37Rv* gene annotation (Rv) of Sanger Institut (http://sanger.ac.uk/projects/M_tuberculosis/Gene_list/). Sheet 2) Proteins identified in replica CFP(1), Sheet 3) Proteins identified in replica CFP(2), both lists including Uniprot identification as obtained in Patternlab for Proteomics, sequence count, spectrum count, number of unique peptides, protein coverage and protein description.

S2 Table. Proteins with predicted signal peptides

Sheet 1) Signal peptide prediction (SignalP 5.0) in *M. tuberculosis* H37Rv reference proteome (UP000001584), Sheet 2) Signal peptide prediction (SignalP 5.0) in *M. tuberculosis* H37Rv CFP, Sheet 3) Proteins in *M. tuberculosis* H37Rv CFP with signal peptides predicted with SignalP 5.0.

S3 Table. Protein abundance comparison against de Souza *et al*, 2011

Comparison of our proteomic data against the proteomic quantitative approach performed by de Souza *et al*, 2011 [13].

S4 Table. Proteins without proteomic annotation in Mycobrowser

Proteins identified in *M. tuberculosis* H37Rv CFP without proteomic annotation in Mycobrowser (Release 3 (2018-06-05)) [33].

S5 Table. Peptides of proteins not previously detected at proteomic level

Sheet 1) Proteins in *M. tuberculosis* H37Rv CFP without previous evidence of expression at protein level, Sheet 2) Scans of peptides confirming proteins identified in *M. tuberculosis* H37Rv CFP without previous evidence at protein level.

S6 Table. Scans of O-glycosylated peptides in *M. tuberculosis* H37Rv culture filtrate proteins

The table includes the File name where the scan was identified, the scan number, peptide charge (Z), measured and theorical mass and the difference (in ppm), scores (primary, secondary, etc), peptide sequence, modification (glycan), glycosylation site p-value, protein and gene data.

S7 Table. O-glycosylation analysis of raw files of Alberthsen *et al*, 2013.

Scans confirming O-glycosylated peptides identified by us in the analysis of the raw data files deposited by Albrethsen *et al*. [37].

A. Relationship between *M. tuberculosis* CFP proteins identified in different studies

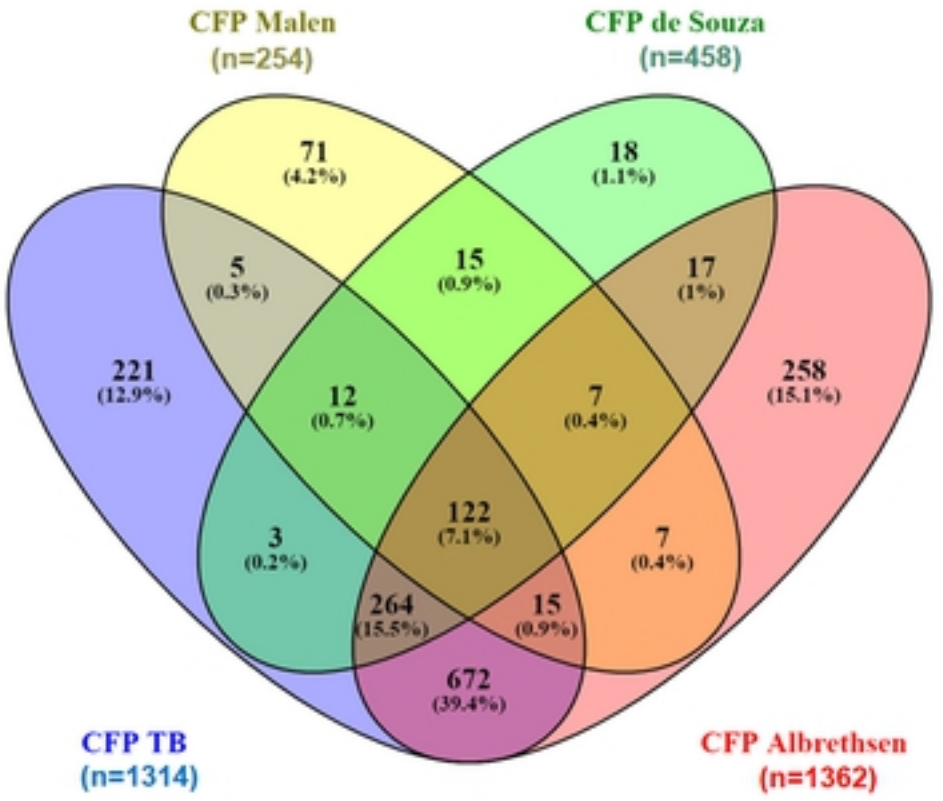

B. Abundance of identified proteins according to number of studies

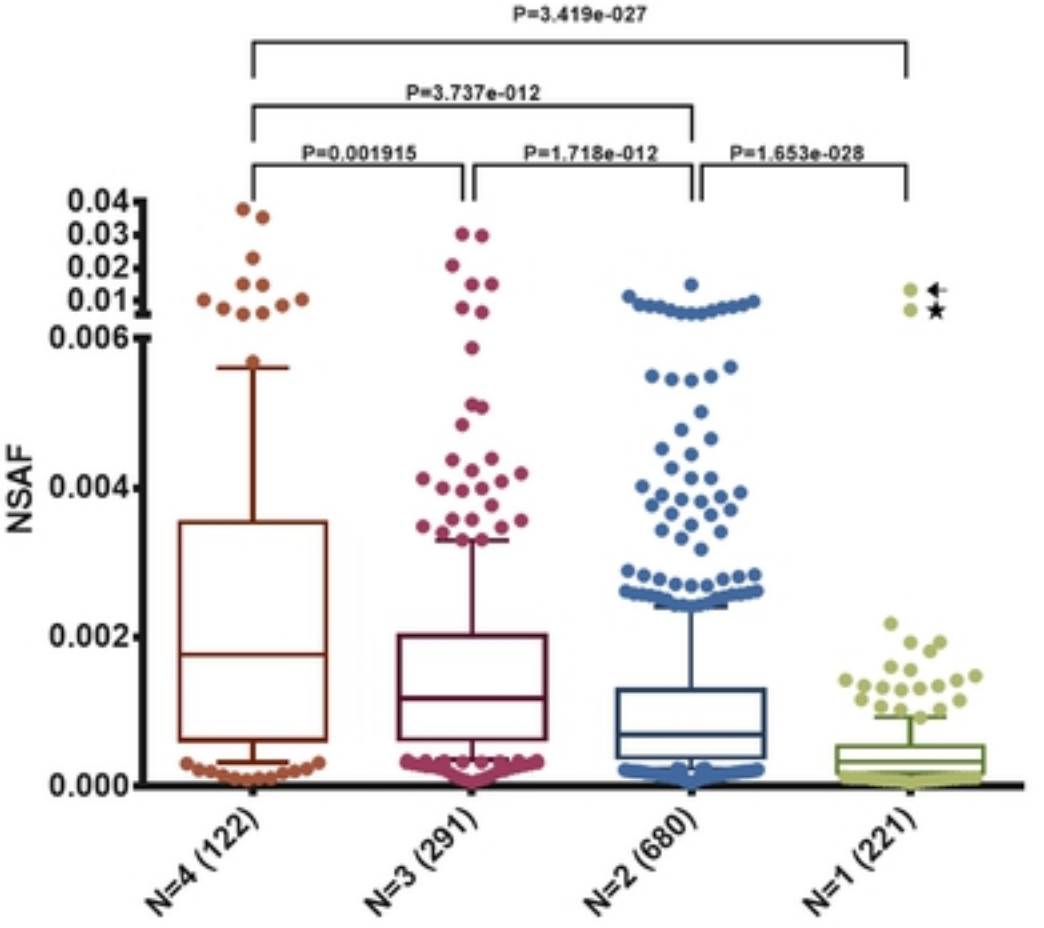

N=4 Proteins identified in this study and in Malen, de Souza and Albrethsen
N=3 Proteins identified in this study and in two other studies comprising Malen, de Souza and Albrethsen
N=2 Proteins identified in this study and in one other study (Malen, de Souza or Albrethsen)
N=1 Proteins identified only in this study

Fig 3

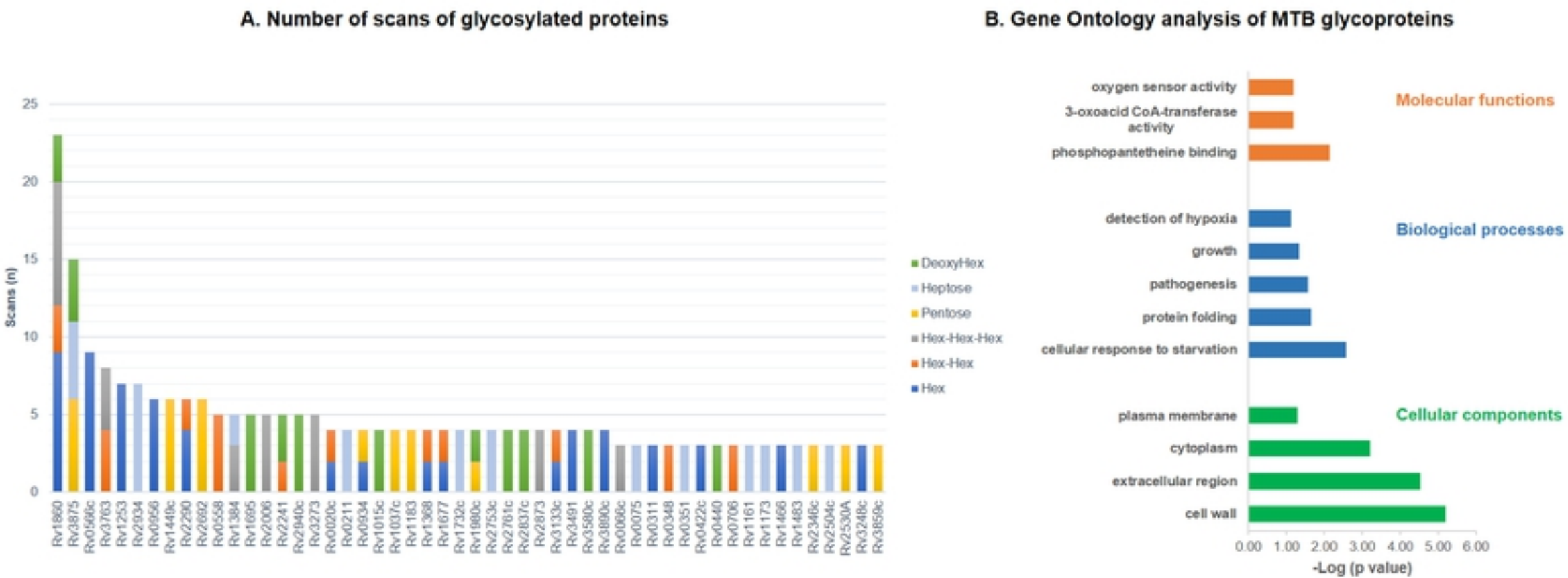
A. Number of scans of glycosylated proteins
Scans (n)
25
20
15
10
5
0
Rv1860
Rv3875
Rv0566c
Rv3763
Rv1253
Rv2934
Rv0956
Rv1449c
Rv2290
Rv2692
Rv0558
Rv1384
Rv1695
Rv2006
Rv2241
Rv2940c
Rv3273
Rv0020c
Rv0211
Rv0934
Rv1015c
Rv1037c
Rv1183
Rv1368
Rv1677
Rv1732c
Rv1980c
Rv2753c
Rv2761c
Rv2837c
Rv2873
Rv3133c
Rv3491
Rv3580c
Rv3890c
Rv0066c
Rv0075
Rv0311
Rv0348
Rv0351
Rv0422c
Rv0440
Rv0706
Rv1161
Rv1173
Rv1466
Rv1483
Rv2346c
Rv2504c
Rv2530A
Rv3248c
Rv3859c
DeoxyHex
Heptose
Pentose
Hex-Hex-Hex
Hex-Hex
Hex
B. Gene Ontology analysis of MTB glycoproteins
oxygen sensor activity
3-oxoacid CoA-transferase activity
phosphopantetheine binding
Molecular functions
detection of hypoxia
growth
pathogenesis
protein folding
cellular response to starvation
Biological processes
plasma membrane
cytoplasm
extracellular region
cell wall
Cellular components
0.00
1.00
2.00
3.00
4.00
5.00
6.00
-Log (p value)

Fig 4

A. EsxA Heptose peptide spectrum

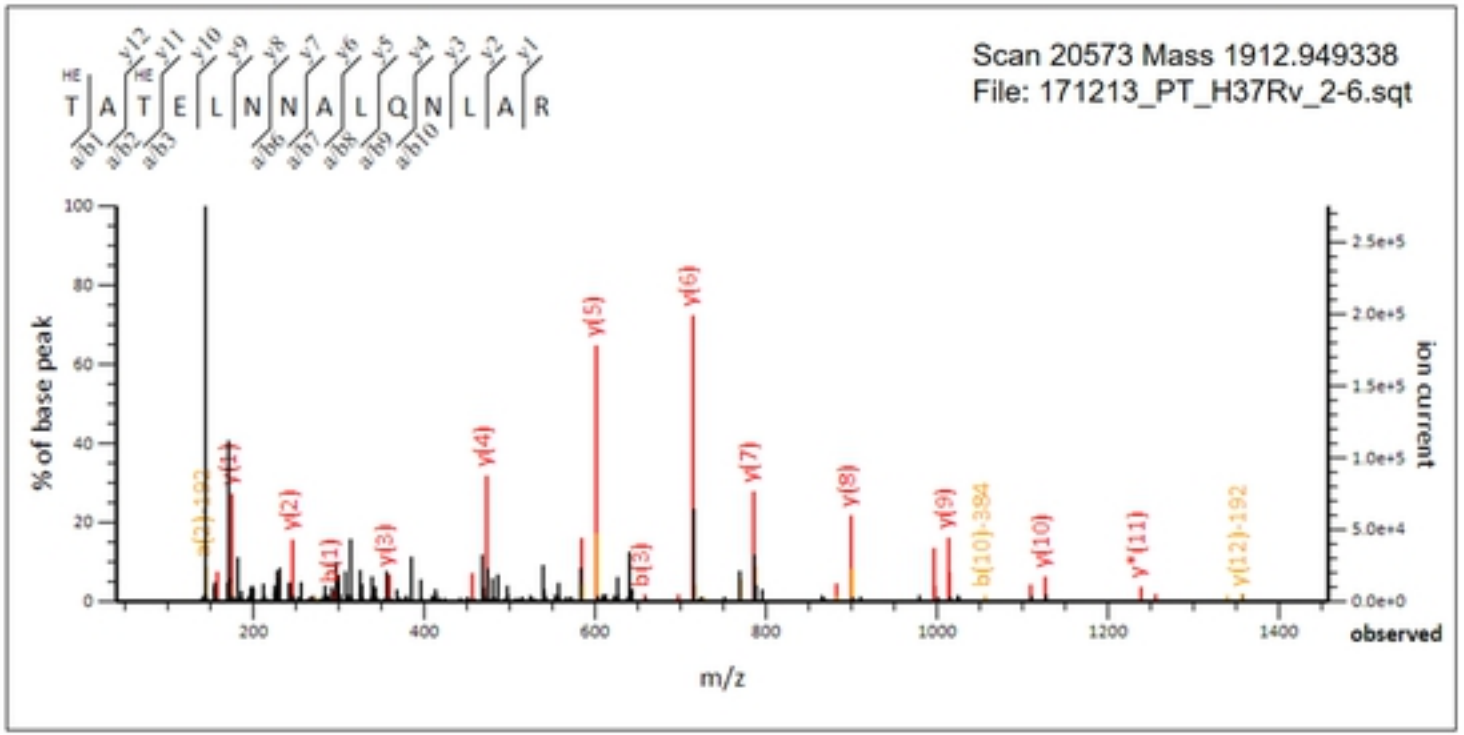

B. EsxA Heptose matched fragment ions

Monoisotopic mass of neutral peptide Mr(calc): 1911.9272
Fixed modifications: Carbamidomethyl (C) (apply to specified residues or ter
Variable modifications:
T1 : Hep (ST), with neutral losses 192.0634(shown in table), 0.0000
T3 : Hep (ST), with neutral losses 192.0634(shown in table), 0.0000
Ions Score: 85 **Expect:** 0.013 (help)

#	a	a*	b	b*	Seq.	y	y*	#
1	74.0600		102.0550		T			14
2	145.0972		173.0921		A	1427.7601	1410.7336	13
3	246.1448		274.1397		T	1356.7230	1339.6965	12
4	375.1874		403.1823		E	1255.6753	1238.6488	11
5	488.2715		516.2664		L	1126.6327	1109.6062	10
6	602.3144	585.2879	630.3093	613.2828	N	1013.5487	996.5221	9
7	716.3573	699.3308	744.3523	727.3257	N	899.5057	882.4792	8
8	787.3945	770.3679	815.3894	798.3628	A	785.4628	768.4363	7
9	900.4785	883.4520	928.4734	911.4469	L	714.4257	697.3991	6
10	1028.5371	1011.5106	1056.5320	1039.5055	Q	601.3416	584.3151	5
11	1142.5800	1125.5535	1170.5749	1153.5484	N	473.2831	456.2565	4
12	1255.6641	1238.6375	1283.6590	1266.6325	L	359.2401	342.2136	3
13	1326.7012	1309.6747	1354.6961	1337.6696	A	246.1561	229.1295	2
14					R	175.1190	158.0924	1

Fig 5

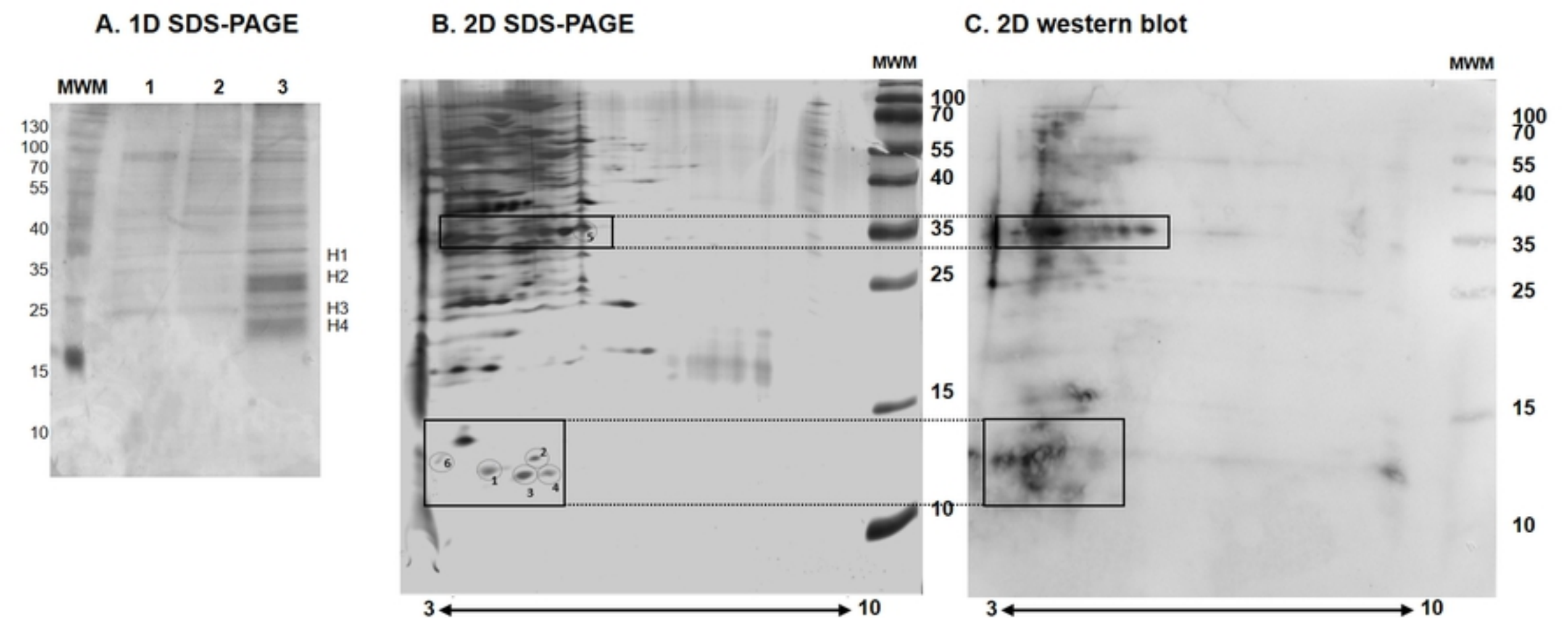
A. 1D SDS-PAGE
MWM
1
2
3
130
100
70
55
40
35
25
15
10
H1
H2
H3
H4
B. 2D SDS-PAGE
MWM
100
70
55
40
35
25
15
10
5
6
1
2
3
4
3
10
C. 2D western blot
MWM
100
70
55
40
35
25
15
10
3
10

Fig 1

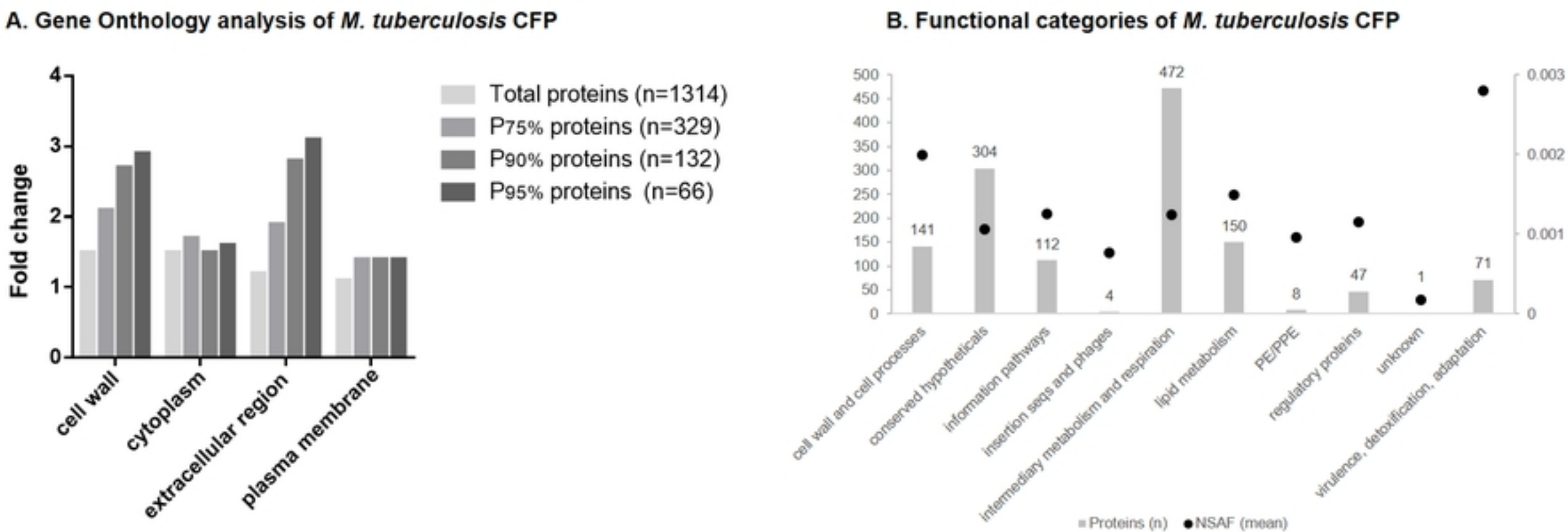
A. Gene Onthology analysis of M. tuberculosis CFP
Fold change
4
3
2
1
0
cell wall
cytoplasm
extracellular region
plasma membrane
Total proteins (n=1314)
P75% proteins (n=329)
P90% proteins (n=132)
P95% proteins (n=66)
B. Functional categories of M. tuberculosis CFP
500
450
400
350
300
250
200
150
100
50
0
0.003
0.002
0.001
0
141
304
112
4
472
150
8
47
1
71
cell wall and cell processes
conserved hypotheticals
information pathways
insertion seqs and phages
intermediary metabolism and respiration
lipid metabolism
PE/PPE
regulatory proteins
unknown
virulence, detoxification, adaptation
Proteins (n)
NSAF (mean)

Fig 2